SAPIENZA
UNIVERSITÀ DI ROMA

Neuroimaging of Language Reorganization in the Preoperative Setting of Brain Tumors

Faculty of Medicine and Psychology
Department of Neuroscience, Mental Health and Sensory Organs (NESMOS)
PhD in Sensorineural Plasticity

Luca Pasquini
Student ID 1715812

Supervisor
Alessandro Bozzao

Co-Supervisor
Andrei I. Holodny

A.A. 2019-2022

OUTLINE

ABSTRACT

Neuroplasticity is extremely relevant in the preoperative setting of brain tumors, due to the potential dramatic consequences of iatrogenic damage to eloquent cortices. The surgical resection of left-hemispheric brain tumors is often complicated by ipsilateral lateralization of language, which is usually localized in the left perisylvian region. Functional MRI (fMRI) is the most widely employed non-invasive method to evaluate language function in the preoperative planning of brain tumors, thanks to its versatility and proven clinical benefits. The implementation of functional connectivity analyses in clinical fMRI can provide new insights about the mechanisms of compensation that the brain develops in response to focal lesions. Language plasticity or reorganization may be associated with tumor growth in the dominant hemisphere for speech preservation against the detrimental effects of neoplastic invasion. Such phenomenon has important effects on patients' outcome and life quality, including the reduction of post-surgical language deficits. In this work we explored language reorganization in the setting of brain tumors, focusing on three specific aims: 1) To demonstrate the existence of language reorganization on fMRI and to identify tumor- and patient-related determinants of language plasticity; 2) To investigate anatomical changes of the cortex in patients with language reorganization by means of structural MRI techniques; 3) To characterize different patterns of language reorganization in brain tumors by means of fMRI, graph theory and intra-operative stimulation. Our results confirmed that tumor growth in the left hemisphere is associated with inter-hemispheric language reorganization, as well as structural modifications of cortical volume in the newly activated areas. Language reorganization appears to be influenced by age, sex, frontal location, Broca's and Wernicke's area invasion, tumor pathology, EGFR amplification, IDH mutation, MGMT methylation, FGFR mutation. Low-grade gliomas show more favorable connectivity changes than high-grade gliomas, in terms of network efficiency and information transfer. Language reorganization develops over time in response to tumor growth or treatments, including surgery, showing progressive recruitment of the right hemisphere. Patients with surgically-proven reorganization display a shift of core language areas to the right side, and demonstrate better language performance compared to the patients who remain left-dominant.

1 INTRODUCTION

The traditional model for language function describes a speech comprehension area in the inferior supramarginal gyrus (SMG) and superior temporal cortex (Wernicke's area - WA), while speech production is ascribed to the inferior frontal gyrus (Broca's area - BA). In more recent years, a growing corpus of research points to a far more complicated organization of the language system. The cognitive processing of language relies on a modular architecture of cortical and subcortical components linked in a widely distributed anatomical connectivity, which includes specific and domain-general networks [1] Herbet et al. proposed a new model for cognitive functions called "hodotopy", which describes language as the result of dynamic communication between eloquent cortices and subcortical white matter bundles [2]. This complex network of interactions can be imaged through magnetic resonance imaging (MRI), with the aid of advanced techniques focused on cortical activations (functional magnetic resonance imaging - fMRI) and axonal connections (diffusion tensor imaging - DTI) [3–5]. In the model proposed by Herbet et al., the brain cannot be described as a mosaic of independent modules, but rather as a graph composed by parallel networks that cooperate in cognitive functioning, and are capable of mutual compensation [2]. The characteristic of mutual compensation represents the center of plasticity, since it allows for brain networks to reorganize in response to localized damage. The first description of brain plasticity was provided by Hebb et al. more than 70 years ago, who demonstrated that coincident neuronal activity can produce structural modifications of the synapses [6]. In the case of language function, functional and structural changes may develop as compensatory mechanisms in response to the damage created by a focal lesion [7–14]

Despite extensive research, the mechanisms and consequences of language plasticity remain largely unknown. For example, different types of focal lesions may cause different patterns of reorganization, depending on their pathology and location in the brain. The timing of a lesion onset is considered to be a crucial variable in the dynamic of reorganization [15]; nevertheless, comparative studies of slow-onset lesions (such as low-grade tumors) vs. rapid-onset lesions (such

as stroke or fast growing tumors) are lacking in the literature. Finally, considerations regarding brain plasticity are often relegated to the domain of neuroscience, with scarce exploration of their clinical impact in the diagnosis and treatment of actual patients. In the presurgical setting of brain tumors, fMRI is primarily used for the assessment of language dominance [16], although it can measure brain connectivity and provide insights on functional networks as well [17]. fMRI appears to be the optimal candidate to investigate language reorganization in the clinical practice, due to non-invasiveness, ability to image the whole brain, and proven clinical benefits [18].

1.1 The Language Network

The human language network can be described from a structural or functional point of view. Understanding the normal organization of language function allows for a better appreciation of plastic phenomena in brain disorders.

1.1.1 The structural language network

There are two main white matter pathways serving the language function in humans: the dorsal stream, responsible for sensorimotor integration, and the ventral stream, related to speech comprehension (Fig. 1) [19,20]. The white matter bundles participating to the dorsal stream include the superior longitudinal fasciculus (SLF)/arcuate fasciculus (AF) system. The AF links the frontal operculum in the inferior frontal gyrus (IFG), aka Broca's area - opercular part (op-BA), and the ventral premotor area (PreMA) to the superior and middle temporal gyri (STG and MTG respectively), including WA. The SLF connects inferior frontal to inferior parietal areas [19,20]. The frontal aslant tract (FAT) links the pre supplementary motor area (SMA) to the IFG, serving verbal fluency [5,21]. Sensorimotor integration culminates in the ventral PreMA and op-BA, which stand at the borders between language cognition and language production serving articulatory planning [22,23]. The ventral PreMA is an important speech production site, due to a close relationship with the anterior-lateral part of the SLF. The integrity of this cortical-subcortical link is essential for speech preservation, representing an anatomical constraint to cortical reorganization [24]. Additionally, Federici et al. described two parallel dorsal pathways through probabilistic DTI. These bundles have

been demonstrated to connect the PreMA to the STG (dorsal pathway I) and the op-BA to the STG (dorsal pathway II), supporting sound-to-motor mapping (dorsal pathway I) and high-level language processing (dorsal pathway II) [25].

The ventral language pathway includes two main white matter bundles: the inferior frontal-occipital fasciculus (IFOF) and the uncinated fasciculus (UF) [19,20]. The former originates from the occipital lobe, connects to the ventral temporal lobe through collateral projections, and terminates in the inferior frontal lobe, including the IFG, the orbital frontal cortex, and the frontal pole. The UF connects the anterior temporal lobe and the inferior frontal lobe [19,20]. Duffau et al. described the IFOF as the primary pathway of the ventral stream, responsible for semantic language processing. The function of the UF in language is instead ancillary, similar to the inferior longitudinal fasciculus (ILF) [26]. The main components of the language network are depicted in Figure 1.

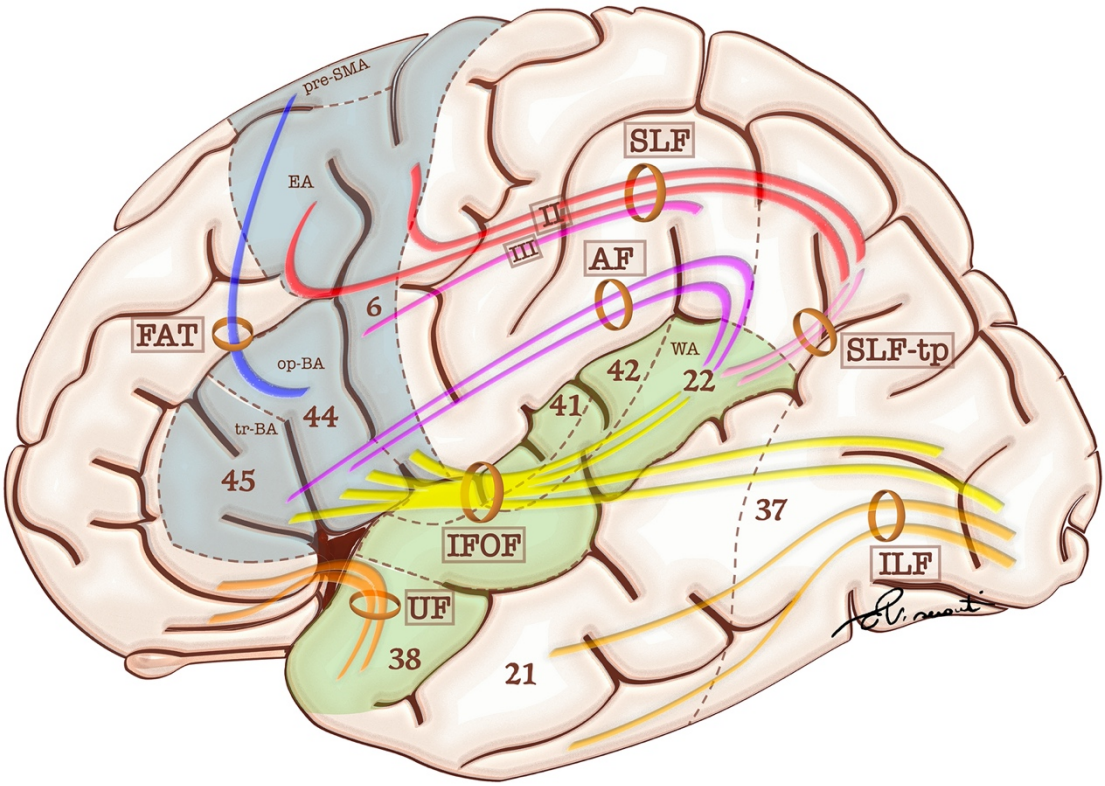

Figure 1. Cortical and sub-cortical components of the language network (from [27])

1.1.2 The functional language network from tb-fMRI

In recent years, the traditional view of language depicting BA and WA as the “expressive” and “receptive” regions of the brain has shifted to new paradigms [28], in consideration of the variability of their localization [1,29], as well as the advancement of network theory. Nevertheless, the localization of eloquent areas prior to surgical procedures retains pivotal importance in clinical practice. The most widely employed non-invasive method to evaluate language function in the preoperative planning is task-based fMRI (tb-fMRI), which uses specific tasks to elicit language-related activations in the brain [16,30].

Visually-administered tasks are characterized by visual cortex activation in the occipital lobe, from which the information reaches Exner’s area [31,32] and the left hemispheric language network [33]. The common architecture of the language network includes BA (traditionally in the pars triangularis and pars opercularis of the IFG), WA (traditionally in the posterior aspect of the STG, variably extending to the inferior parietal lobule), and SMA (commonly located in the superior-medial frontal gyrus) [34]. The PreMA (Brodmann’s area 6) is located in the dorsal-lateral pre-frontal cortex (DLPFC), including Exner’s area in posterior aspect of the middle frontal gyrus (MFG). EA is important for handwriting, participating to the transformation of phonological representations of words into motor commands [31], but it is also involved in naming [35] and reading [36]. The frontal eye field is another part of Brodmann’s area 6, which coordinates voluntary and saccadic eye movements, visual field perception and awareness [37]. In visually-administered tasks based on written paradigms, activation of the visual word form area (VWFA) in the inferior temporal gyrus (ITG) can be noted. The VWFA elaborates visual information by integrating inputs from the occipital cortex [38,39], participates in visual and auditory naming, auditory comprehension, repetition, and spontaneous speech [33]. Fusiform gyrus activation is also expected in visual tasks which include face recognition[40]. On the other hand, auditory tasks are characterized by the activation of the auditory cortex located in the Heschl’s gyrus (primary auditory cortex) [41], which replaces the role of the visual cortex as input source for the language network.

Secondary language areas can be found in the temporal lobe, angular gyrus, left insula, anterior cingulate cortex, basal ganglia, hippocampus, and cerebellar hemispheres [42–46]. These areas are often considered expendable in the surgical planning of brain tumors resection [38]. Due to the implications of surgical interventions in the vicinity of eloquent cortices, the concept of hierarchical organization of language areas assumes particular relevance in clinical practice. Graph-theory applied to fMRI can help to identify “core” language areas whose integrity is essential for the stability of the network [47–49]. Previous studies have demonstrated that SMA, PreMA, and BA form a frontal “core” of the language network [47], which appears consistent in the healthy population regardless of the spoken language [50].

1.2 The plastic potential of the brain

Brain plasticity encompasses two different phenomena: 1) Functional plasticity, which consists in the modification of synaptic strength with no changes of anatomical connectivity in between; 2) Structural plasticity, which implies anatomical modifications. The former phenomenon takes place at the synaptic level, with persistent strengthening or weakening of synapses based on recent patterns of activity, defined as long term potentiation (LTP) or depotentiation (LTD) [51,52]. Structural plasticity may manifest as synaptic rewiring, in which existing synaptic connections are swapped, or as de novo synaptogenesis. Structural changes may also include retraction and reformation of dendritic spines, re-routing of axonal branches [53], or synaptic pruning, which consists in the elimination of less effective synapses to prioritize most productive connections [54]. Axonal sprouting is described as the formation of new physical connections between neurons, while myelin plasticity includes the variation of oligodendrocyte proliferation/differentiation, nodal or internodal length, as well as myelin remodeling [55]. Finally, neurogenesis can be considered another form of structural plasticity, although it predominantly takes place in the early life [56,57]. Structural and functional plasticity are closely related to each other: the activity of a neuron, whether spontaneous or experience-driven, can lead to the formation of new synapses. Transmitter release

in intensely activated areas may promote synaptogenesis and rewiring [58]. Similarly, changes in synaptic number and/or morphology may be associated with LTP/LTD [52].

Microscopic changes related to structural an functional-plasticity translate to macroscopic modifications of brain anatomy and function, which can be observed with MRI. Microscopic changes of neurovascular units may affect regional blood flow and oxygenation, which are detected by fMRI as fluctuation of blood oxygen level dependent (BOLD) signal. In the normal brain, neurons can regulate the cerebral blood flow (CBF) by means of specific signals directed to local endothelial cells. Glutamatergic synaptic activity leads to a neurotransmission cascade directed toward the activation of neuronal NO synthase (nNOS) and cyclooxygenase 2 (COX-2). These enzymes produce potent vasodilators [59], which act on regional blood vessels. Glutamate also participates in LTP, which represents the main manifestation of functional plasticity at the microscopic level [60]. From these considerations, it appears realistic that microscopic changes in synaptic function may translate into modifications of fMRI activation. Enhanced activity and learning of new functions may produce structural plasticity of the cortex, possibly reflecting synaptic rewiring or synaptogenesis [61,62]. Cortical volume or thickness can be detected by MRI through images routinely acquired in the clinical practice, such as volumetric T1-weighted sequences [63]. Myelin plasticity, axonal sprouting or rewiring modify the diffusion properties of brain tissue and can therefore be studied with DTI or NODDI [64,65].

Neuroplasticity induced by focal lesions can be explained starting from cortical inhibition. During the development plasticity is required to establish normal brain functions. The inhibitory activity of GABA interneurons builds up to a specific time window in early life – the “critical period” (CP) – when physiologic plasticity may occur. In the adult life, the intraneuronal inhibitory activity keeps growing until it overcomes the threshold of CP, creating a new equilibrium to protect established neural circuits from undesired changes, as well as stored memories and learned skills [66,67]. As a consequence of this process, cortical inhibition is predominant in the adult brain, with most activity occurring in less than 10% of viable neurons [68]. Focal injuries cause cell death and synaptic loss, which primarily targets the inhibitory interneurons due to their large prevalence. The

result is a decrease in GABAergic output, leading to increased excitability, neurite expansion, and synapse formation [69]. Cortical disinhibition creates a permissive environment for the activation of nearby circuits, allowing for plastic phenomena to take place [67]. When a focal lesion invades eloquent cortices, it causes disinhibition of nearby neural networks, possibly leading to adaptive plasticity. In the case of language, healthy right-handed subjects normally show left hemispheric dominance (91–96%), with a small percentage of native co-dominant or right dominant (atypical dominance) [70,71]. If the left dominant hemisphere is invaded by a focal lesion such as a stroke or a tumor, the brain may be able to reorganize the language function to overcome clinical deficits. These plastic changes may manifest with the recruitment of surrounding regions (intra-hemispheric reorganization) [72], or by translocation of language areas to the right hemisphere (inter-hemispheric reorganization), probably via disinhibition of the corpus callosum [53,73]. A summary of the neurobiology of language reorganization is depicted in Figure 2.

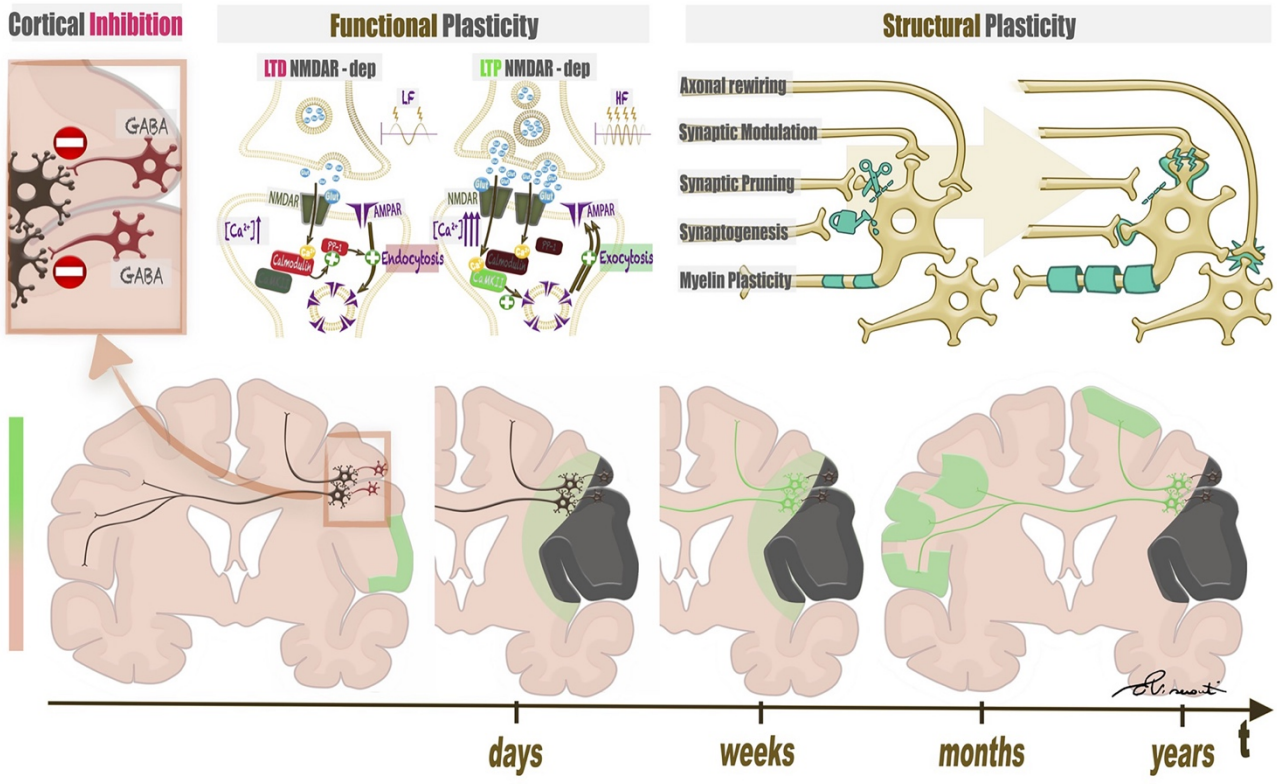

Figure 2. Mechanisms of functional and structural plasticity (from [27])

1.3 Language Reorganization in Focal Lesions – Functional Plasticity in Brain Tumors

Prior studies based on resting state fMRI (rs-fMRI) have demonstrated that both low-grade gliomas (LGG) and high-grade gliomas (HGG) can modify the functional connectivity of the language network, producing long-range effects on the right hemisphere [74]. The measure to which such alterations achieve compensation of clinical deficits (adaptive plasticity) is still unclear. Language reorganization appears to be affected by tumor pathology [75] and genetics [76], since less aggressive behavior may allow for the brain to develop the required anatomical and functional modifications. Also, lesion location near 'connector' regions, important areas for information transfer among sub-networks, causes greater effects than damage to peripheral areas [42,77].

The reorganization of language in the setting of brain tumors has been described to follow a progressive pattern: within due time, intra-tumoral activation shifts to perilesional areas [15,78], thus leading to the recruitment of contralateral homologues [7,8,14,79–81]. According to this theory, the pace of growth of tumoral lesions plays a crucial role in the development of functional reorganization [82]. The initial manifestation of language plasticity includes the recruitment of peritumoral and homolateral cortices [15]. This process has been described in non-aphasic patients with gliomas invading BA, whose language activation may extend to the left peritumoral inferior frontal cortex [83]. In a similar way, left insular tumors may show perisylvian compensatory activation [84]. Patients with left hemispheric tumors demonstrate increased activation of the left DLPFC, frontal-orbital cortex, anterior insula, and left cerebellum compared to the healthy population [85]. The invasion of BA from LGG is associated with the activation of the left insula, premotor cortex, and frontal-orbital cortex [86]. As final step of language reorganization, a widely distributed network of eloquent cortices can be recruited in the contralateral hemisphere. This process includes the right-translocation of BA[8,14,79] or WA [7,87], which is also referred to as activation of right-sided BA or WA homologues. Rosenberg et al. described the change in language lateralization from left to co-dominance in a right-handed patient with left hemispheric LGG during a 2-year timeframe before surgical intervention [81]. An example of inter-hemispheric language reorganization is depicted in Figure 2.

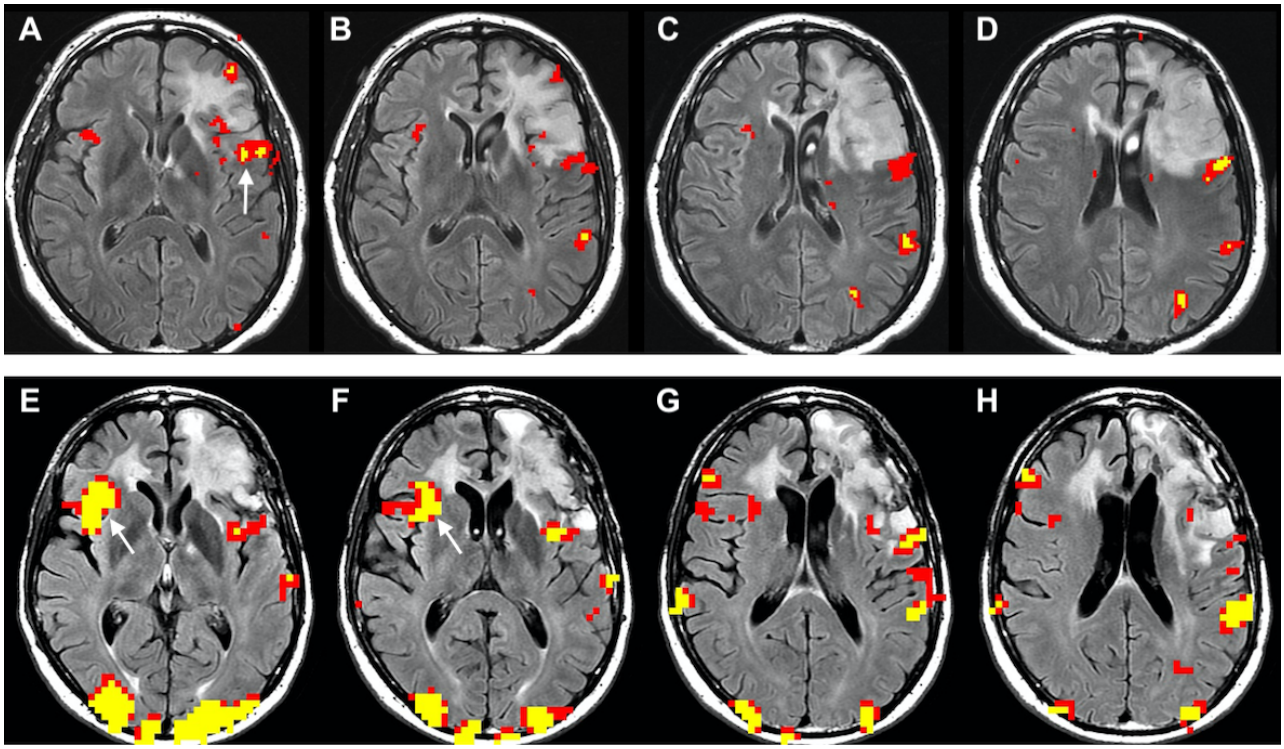

Figure 3. Inter-hemispheric language reorganization in a right-handed patient with LGG invading the left inferior frontal gyrus. The images above (A–D), obtained before surgery, show peritumoral functional activation in the expected location of Broca's area (white arrow in A). The images below (E–H) were obtained 4 years after the surgery. A new strong functional activation is visible in the right hemisphere, corresponding to Broca's area homologue (white arrow in E and F).

Brain connectivity analyses can provide additional information to enrich our understanding of language plasticity. In the study by Li et al., network modifications associated with right translocation of BA were described in a patient undergoing surgery for left-hemispheric LGG [14]. As opposed to the normal connectivity of a healthy brain, the newly activated right BA homolog displayed an indirect connection to the left WA through the SMA and the MFG [14]. Cho et al. analyzed the reorganization of cerebral-cerebellar networks in right-handed patients with left frontal gliomas [88]. The described reorganization of these networks consisted in the development of left-sided activity in the cerebellum VI segment, in place of the expected crossed activation, confirming an earlier report by Thiel et al. [85]. Zhang et al. showed a similar reorganization of cerebral-cerebellar language circuits in response to tumoral invasion by LGG and HGG [89]. Of note, LGG patients displayed cortical volume

changes in regions with increased brain activity, as per structural-functional coupling [89]. Despite most studies focused on LGG-induced plasticity, few cases of inter-hemispheric reorganization in HGG have been reported in the literature [7,8,79]. This may support the idea that language reorganization can develop in any infiltrating tumor, irrespective of the grade. Nevertheless, the topic remains a matter of debate.

The adequacy of right-sided language areas in providing a reliable function – aka effective compensation - is still debated. Some evidence from prior studies supports a better clinical performance in patients with functional modifications consistent with reorganization [42,79,90]. Right-sided language areas proved to be functional by eliciting speech deficits when stimulated with trans-cranic magnetic stimulation (TMS) [9,91]. Experiments with TMS-induced 'virtual-lesions' demonstrated left hemispheric dominance in healthy subjects, while co-dominance was reported in brain tumor patients, characterized by the presence of language errors in both hemispheres [92]. In agreement with these findings, several studies reported complete recovery after resection of well-known eloquent cortices due to tumor invasion [93–95]. Conversely, the presence of right-sided activation has not always been associated with better clinical performance [9,96,97].

Notably, there are reports describing that surgery itself can induce plastic changes. In the post-operative setting, perilesional activation is essential for language recovery [98]. Post-surgical reorganization to nearby areas has been described by prior authors, for example in the case of the left lingual gyrus taking over the function of the left parahippocampal gyrus in a picture-naming task [99]. Surgical resection of BA has been associated with the recruitment of adjacent regions, in particular the ventral premotor cortex, IFG – pars orbitalis, DLPFC, and insula. These modifications were also associated with better post-surgical outcomes [100]. Insular tumors may lead to the activation of the frontal and temporal operculum, as well as of the left putamen [15,101]. Resection of WA has been associated with the recruitment of the surrounding cortex and the progressive involvement of remote areas, including the left SMG, IFG - pars triangularis, as well as the activation of contralateral homologues [95]. Finally, SMA resection may activate the contralateral homolog and the premotor cortex [102,103]. Post-surgical language reorganization appears to be related to

cognitive improvement, in a similar way as after glioma resection [104], although the topic remains debated.

1.4 The Preoperative Planning of Brain Tumors

fMRI is an advanced imaging technique capable of measuring BOLD signal associated with brain activity through the detection of changes in local blood flow to the brain cortex [105]. The main application of fMRI in neuro-oncology is the pre-operative planning of patients with brain tumors [16,105,106]. In brain tumor surgery, it is essential to perform radical resection of the tumor to improve survival [107], while preserving the adjacent eloquent areas to minimize postsurgical deficits. The essential roles of fMRI include: 1) to plan the surgical approach for resection; 2) to define the relationship of brain lesions to eloquent areas in the preoperative setting; 3) to assess for the need of intraoperative cortical stimulation (ICS) and to plan the cortical mapping; 4) to determine language dominance; 5) to help identifying crucial anatomical landmarks such as the precentral (motor) gyrus. Furthermore, fMRI can complement ICS findings and balance its drawbacks and limitations. During ICS, the patient is woken from general anesthesia and asked to perform specific tasks to assess brain functions related to the stimulated cortex. A correct ICS procedure requires patient extubation, which reduces the control over blood oxygenation levels, and adequate compliance. Furthermore, minimum positive thresholds for stimulation events during ICS may show intra- and inter-subject variability and a certain degree of dependency from the electrode intensity [108]. Similarly, the ability of ICS to reproduce interferences over several trials depends on the patient's baseline error rate, which is expression of the patient's clinical state [108]. As a consequence, ICS mapping alone may not be sufficient to confidently define surgical margins in some occasions. Conversely, preoperative fMRI can decrease unexpected events during surgery, reduce time of operation and anesthesia, support ICS findings and provide complementary information in case of ICS failure [109,110]. The most widely used method to pre-operatively evaluate language and motor functions is task-based fMRI (tb-fMRI), which relies on specific functional tasks to localize brain function and to guide surgical resection [111]. The inclusion of fMRI

in the neuro-oncologic pre-operative planning has clear and established clinical benefits. Luna et al. recently demonstrated the decrease in post-operative complications from 21% to 11% in patients who underwent fMRI as part of their pre-operative planning [112].

2 SPECIFIC AIMS

The work of this thesis was focused on the exploration of tumor-induced language reorganization. Through the following specific aims (SA) and experiments we wanted to expand the current understanding of neuroplasticity, including its neurobiological mechanism and associated factors. The overall goal of the present work was to improve the preoperative planning of brain tumors by incorporating information on plastic phenomena in order to guide therapeutic approaches and future targeted therapies. In the following paragraphs the overall goal of the thesis is broken down to three main SA. The methods and results sections will address each SA individually. The discussion section will explore the meaning of the main concepts emerged from our results.

2.1.1 SA#1: To demonstrate language reorganization in brain tumors with fMRI and to identify tumor- and patient-related determinants of language plasticity

Among healthy subjects, 91–96% of right-handed individuals and 73–75% of left-handed individuals are left-hemispheric dominant for language [70,71]. Language reorganization may develop as a possible compensatory mechanism in response to tumor invasion of the dominant hemisphere, leading to changes of language dominance [27]. Although there is evidence of language reorganization in many processes including brain tumors, the precise dynamics remain elusive. Many studies on tumor-induced language reorganization are based on low-grade gliomas [113,114]; however, even fast-growing tumors may display a life-cycle compatible with the timeframe of brain plasticity [115], as demonstrated by neurobehavioral studies [61,62,116]. Tumor genetics/molecular anomalies describe tumor behavior and likely influence reorganization [76], since a less aggressive behavior and slower-paced growth may facilitate plasticity. Also, tumor location effect on plastic phenomena is poorly explored. The location of a lesion likely influences the outcome of

reorganization: damage to brain regions important for communication between subnetworks (connectors) causes greater effects than the damage inflicted to peripheral areas [77].

In our first SA we investigated the effect that patient age, handedness, and sex, as well as tumor location and molecular features, have on fMRI language laterality. We studied the relationship between each of these variables and five laterality indexes (LI) calculated in the frontal lobe, Broca's area (BA), temporal lobe, Wernicke's area (WA), and whole cerebral hemisphere. The hypothesis related to SA#1 were the following: 1) Patients with left-hemispheric brain tumors would display more-than-expected right-hemispheric participation in language function compared to what has been previously reported in the healthy population; 2) Tumor involvement of eloquent language areas and favorable genetics would be associated with language reorganization.

2.1.2 SA#2: To investigate anatomical changes of the cortex in patients with language reorganization by means of structural MRI techniques

Functional modifications of the language network may be associated with structural changes of the newly activated brain regions, since the implementation of a function has direct effects on the number of synapses in the relative cortex [58]. This hypothesis has been proven true by showing learning-dependent increases in cortical volume of brain areas related to linguistic, procedural, spatial orientation, and navigation abilities in healthy subjects [61,116,117]. A seminal study from Labudda et al. investigated structural correlates of inter-hemispheric language reorganization in epileptic patients [10]. The authors demonstrated that patients harboring left hemispheric epileptic foci show increased cortical volume in the right hemisphere. Similar modifications can be hypothesized for brain tumors; however, this idea has never been explored.

In our second SA we investigated structural correlates of functional reorganization by assessing whether atypical language dominance in patients with left inferior frontal and insular glioma is associated with areas of increased of cortical volume in the right hemisphere. The hypotheses related to SA#2 was that inter-hemispheric language plasticity, as depicted by atypical language organization, would be associated with increased cortical volume in areas of known

language function in the right hemisphere, including the right-sided Broca's and Wernicke's homologues.

2.1.3 SA#3: To characterize different patterns of language reorganization in brain tumors by means of fMRI, graph theory and intra-operative stimulation

Historically, the brain has been described as a mosaic of multiple areas, each related to a specific function. This concept is known as localizationism. However, modern neuroscience suggests that the brain is actually organized as a network [118] and that cognitive processes arise from the dynamic interaction of network components [2]. Evidence to support this theory is provided by neuroimaging studies, especially those that focus on the language system. The historical model of language function, localizing speech comprehension in the superior temporal gyrus (Wernicke's area) and speech production in the inferior frontal gyrus (Broca's area), has changed over time [1]. Duffau et al., among others, demonstrated over many years that surgical resection of brain tumors that invade eloquent brain areas is feasible with limited postsurgical deficits [82]. The original location of Broca's area has been reviewed and extended to include a penumbra of brain tissue surrounding the inferior frontal gyrus and leading to negative speech responses during ICS [28]. Presurgical fMRI using post-processing techniques and computational models have supported the network theory [119,120]. Connectivity analyses, especially those relying on graph theory, can provide additional information concerning the relationship between eloquent cortices. These techniques aid in the identification of fundamental network components (core) and have important clinical implications for the neurosurgeon who wants to achieve maximal resection while sparing crucial eloquent areas [47–49]. Specific graph-theoretical measures can be used to characterize the effect on brain networks of tumors with different grade and location [121]. Graph theory can also highlight core components of a network by testing their stability through the progressive removal of connections [122]. This technique has been used to show that the pre-supplementary motor area, premotor cortex, and Broca's area are part of a frontal core of the human language network [47] that is tightly connected to Wernicke's area and appears consistent in healthy subjects regardless of their spoken language [123].

In our third SA we explored language reorganization through graph theory to shed light on brain connectivity modifications related to the presence of a tumor in the dominant hemisphere. For this purpose we conducted three experiments: 1) We studied the network modifications of 30 left-hemispheric LGG and 30 HGG versus 20 healthy controls (HC) by applying graph-theory to resting-state fMRI. Our objective was to compare the network modifications in the whole brain, single hemispheres and single lobes induced by tumors of different grade (LGG vs. HGG) and location with respect to HC. 2) We explored the functional reorganization of language over time before and after surgery in a prospective cohort of 5 left-hemispheric LGG patients, using longitudinal task-based fMRI, graph-theory, and language assessment. We analyzed functional connectivity patterns to explore network modifications underlying language reorganization. 3) We employed fMRI and graph-theory to investigate the functional language network of 44 patients with left-hemispheric LGG and IOS-proven language reorganization during awake surgery. We compared the architecture of the core language network as defined in Li et al. [47] between patients with speech arrest (SA) and no speech arrest (NSA) during surgery.

The hypotheses related to SA#3 were the following: 1) In the first experiment, HGG would display predominant regional modifications due to neurovascular uncoupling, while LGG would demonstrate both ipsi- and contralateral changes suggestive of reorganization. We also hypothesized LGG networks to be more integrated and connected than those of HGG, possibly reflecting a better clinical performance. 2) In the second experiment, patients with LGGs would show increased activation of right-sided language-related areas over time on fMRI (increased right laterality), while graph-theory would demonstrate increased connectivity of right-sided language-related areas and increased inter-hemispheric participation in language. 3) In the third experiment, language reorganization in NSA patients would be associated to a modification of the core language network compared to SA patients and healthy subjects. We also hypothesized that network changes in NSA would be associated with better language performance.

3 MATERIALS AND METHODS

3.1 Patients

We reviewed the imaging archive of Memorial Sloan Kettering Cancer Center from January 2012 to February 2022, and selected patients with brain tumors according to specific inclusion criteria for every objective. Clinical charts were reviewed to obtain patients' demographic information, including age and sex. Handedness was established through the Edinburgh Handedness Inventory [124]. The institutional pathology archive was reviewed to gather information about tumor diagnosis, grade (World Health Organization classification 2021 or prior), and molecular data, including O(6)-methylguanine-DNA methyltransferase (MGMT) promoter hypermethylation, isocitrate dehydrogenase (IDH) mutation, epidermal growth factor receptor (EGFR) amplification, and fibroblast growth factor receptor (FGFR) mutation. Molecular data was obtained through the Integrated Mutation Profiling of Actionable Cancer Targets test (MSK-IMPACT™), as explained in prior publications [125]. The location of every tumor was annotated based on MRI to include anatomical areas (frontal, temporal, parietal, and occipital lobes; insula; and cerebellum), as well as eloquent areas of the language network (BA, WA, Exner's area, SMA, SMG, and angular gyrus - AG). Patients' language performance was assessed preoperatively with the Boston Naming Test (BNT) [126]. Furthermore, we retrospectively reviewed individual clinical charts to gather information about the presence of speech deficits in the neurologic objective examination performed before surgery, within 1 week after surgery, and three-to-six months after surgery.

The patients recruited for the prospective cohort study (SA#3 Experiment 2) underwent additional language testing at every timepoint, including: BNT [126], Phonemic Verbal Fluency (PVF) and Category Fluency (CF) Test [127].

Specific inclusion criteria were adopted to pursue each one of our SAs, as follows:

- SA#1: Left-hemispheric brain tumors; no tumor involvement of the right hemisphere by either multifocal tumor or direct extension; availability of language tb-fMRI; absence of tumor-related or patient-related artifacts, including drop-out from hemorrhagic components, prior surgery, or

head motion; absence of prior brain insult (i.e. stroke) or brain disease other than tumor. We evaluated 405 patients for this objective.

- SA#2: Left inferior frontal and/or insular tumor; no tumor involvement of the right hemisphere by either multifocal tumor or direct extension; availability of language tb-fMRI and high-resolution 3D T1 weighted images; absence of tumor-related or patient-related artifacts, including drop-out from hemorrhagic components, prior surgery, or head motion. We evaluated 127 patients for this objective.
- SA#3, experiment 1: Newly diagnosed left-hemispheric glioma (World Health Organization 2016 classification [128]); no prior surgery or other treatment; resting-state data acquired with the same protocol and therefore comparable; absence of tumor-related or patient-related artifacts including drop-out from hemorrhagic tumor components and motion. We evaluated 60 patients and 20 healthy subjects for this objective.
- SA#3, experiment 2: Newly-diagnosed left-hemispheric glioma undergoing surgery; pathologic diagnosis of LGG at first biopsy; right-handedness; absence of tumor-related or patient-related artifacts including drop-out from hemorrhagic tumor components and motion. Patients were followed with longitudinal tb-fMRI and clinical language assessment prior to tumor resection (baseline) and at three intervals after surgery: post-op1 (4-8months), post-op2 (10-14months), post-op3 (16-23months). We evaluated 5 patients for this objective.
- SA#3, experiment 3: Patients with left-hemispheric LGG; peri-sylvian location; availability of language tb-fMRI; absence of tumor-related or patient-related artifacts, including drop-out from hemorrhagic components, prior surgery, or head motion; awake surgery with intraoperative mapping results; speech deficit evaluation at the time of surgery (by neurologic exam).

3.2 MRI Protocol

MR scans were acquired on a 3.0 T GE magnet (General Electric, Milwaukee, WI) with an 8-channel head coil. Functional matching anatomical T1-weighted (repetition time (RT), 600 ms; echo time (ET), 8 ms; thickness, 4.5 mm) and T2-weighted (RT, 4000 ms; ET, 102 ms; thickness, 4.5 mm)

spin-echo axial images were acquired for every patient and co-registered with functional data. 3D-T1-weighted anatomical images were acquired with a spoiled gradient recalled sequence (RT/ET, 22/4ms; matrix, 256×256; thickness 1 mm). Tb-fMRI was acquired with gradient-echo echo-planar imaging (RT, 2500ms; ET, 30); matrix, 64×64; field of view, 240 mm; thickness, 4.5 mm; flip angle 80°, 34-36 slices covering the whole brain). Head motion was minimized using straps and foam padding. During the tb-fMRI acquisition, subjects performed a phonemic fluency task (letter) tailored to match a block paradigm of 8 cycles alternating activation phases of 20 sec with resting phases of 30 seconds. In the activation phase, letters on a neutral background were displayed visually to the subjects. During the resting phase, patients were asked to fixate a crosshair image. The language task itself consisted in the silent generation of words that began with the presented letter (for example: subject presented with the letter “A” may generate words such as ‘apple’). All tasks were delivered visually with a dedicated system (Resonance Tech, CA). The fMRI sequence consisted of 160 volumes of 32 images covering the entire brain. Subjects’ performance and real-time generated language activity were monitored at the acquisition console with dedicated software (Brainwave RT, GE Healthcare, Milwaukee, Wisconsin). Rs-fMRI was acquired with single-shot gradient echo EPI (TR/TE=2500/32 ms, section thickness=4mm, matrix=64x64mm, FOV=240mm, acquisition volume = 160, scanning duration=6minutes 55 seconds), while the patients were asked to rest in the scanner.

3.3 Intra-operative Stimulation (IOS)

Patients selected for speech mapping underwent awake anesthesia [129]. After the craniotomy was performed and the appropriate brain region exposed, speech mapping was performed. A surgical navigation software (BrainLab GmbH, Munich, Germany) was used as per routine, and the functional MRI data was uploaded to the workstation used for the surgical navigation. A neurophysiologist was present during the procedure and was responsible for the EEG and other neurophysiological readings. An assistant sat next to the patient and performed the speech testing. In most cases, SSEPs (Somatosensory evoked potentials) were performed indicating the location of

the central sulcus. The location of BA was approximated based on a combination of factors including expected anatomic location in the operculum, fMRI findings and extrapolation from the location of the central sulcus. The inferior frontal gyrus at the operculum was then subject to direct cortical stimulation using a bipolar probe and starting at 4 mA and up to a maximum of 14 mA. The patient was asked to count or to cite the alphabet while the brain was being intermittently stimulated. Electro-corticography was carried out simultaneously via a surface electrode, to monitor for seizure activity or after-discharges. Speech arrest was defined as complete stopping of speech, with preserved tongue movements, reproducible at least three times and occurring immediately following electrical stimulation of the same cortical surface area. If speech arrest was not obtained, the area being stimulated was expanded to include most of the inferior frontal gyrus, up to the middle frontal gyrus and posteriorly towards the sensorimotor strip, depending on the extent of the craniotomy.

3.4 Functional Analysis through fMRI and Graph Theory

In the following paragraphs we describe the fMRI analysis workflow related to SA#1, 2 and 3. As detailed below, we employed Task-based fMRI to calculate language dominance and to build individual language networks through optimal percolation [48]. We used rs-fMRI to build hemispheric and lobar networks, and to calculate graph-theory efficiency measures related to small-worldness and information transfer (brain connectivity analysis). Study groups and statistical comparisons are described in the statistics section (3.6).

3.4.1 Assessment of Language Dominance on Task-Based fMRI

Functional data was processed using Analysis of Functional NeuroImages (AFNI) [130]. We corrected head-motion artifacts by using 3D rigid-body registration based on a reference volume acquired at the beginning of each examination. Subsequent steps of the post-processing pipeline included: 1) Spatial smoothing through a Gaussian kernel with full width at half maximum of 4mm; 2) Removal of linear trend and high-frequency noise; 3) Generation of statistical parametric maps from stimulus-locked responses by cross-correlating a modeled waveform corresponding to the

block paradigm with all pixel time courses on a pixel-by-pixel basis. Voxels with standard deviation exceeding 8% of the mean signal intensity were set to zero to minimize false positives.

Multiple LI were calculated from tb-fMRI maps through a threshold-independent method by using different ROIs [131,132]. The workflow for LI calculation included: 1) Nonlinear registration (ANTS) of 3D T1-weighted and functional images to MNI152 standard space. The registration of functional images was based on the first volume of the echo-planar sequence and applied to the correlation maps generated after post-processing; 2) Co-registered 3D T1-weighted images were parcellated in multiple cortical regions based on the automated anatomical labeling (AAL) atlas; 3) The mean value of the 5% most-activated voxels on the correlation map was calculated for every subject; 4) A threshold of above 80% of this mean was applied to select voxels for each region of interest (ROI) used to calculate the LI; 5) The traditional formula LI=(L-R)/(L+R) was applied, where L and R represent the number of voxels in the left and right ROI, respectively. We calculated five LI corresponding to the following ROIs: cerebral hemisphere - excluding cerebellum and visual cortex, temporal lobe, frontal lobe, BA, WA. The results were confirmed by comparing LI values with the respective fMRI maps overlayed on 3D-T1 images.

3.4.2 Individual Language Network Analysis through Optimal Percolation

Individual functional language networks were obtained from tb-fMRI by using functional ROIs corresponding to active clusters and by applying optimal percolation thresholding, as shown in previous publications [47,48,123,133]. In summary, contiguous active voxels in the same anatomical regions were labeled as belonging to the same functional ROI. Functional links were inferred by thresholding pair-wise correlations between voxels with a penalization parameter set to optimize brain integration (all the clusters are connected) and sparsity (minimal wiring) [48]. Optimal percolation thresholding is based on biological evidence of neural architectures, and demonstrated promising results in identifying most important connections in brain networks [47,133].

Changes of hemispheric connections were quantified with a ‘Connectivity laterality Index’ (CI), based on weighted values from connectivity matrices to account for connection strength, and calculated with the formula: $(WC_L)/(WC_L+WC_R)$, where WC_L=total weight of left hemispheric links,

WC_R=total weight of right hemispheric links. The CI values can range between 0 (only right hemispheric connections) and +1 (only left hemispheric connections), with 0.5 representing perfectly balanced connections between the two hemispheres. The analysis was conducted in Matlab (R2017a, Massachusetts: The MathWorks Inc).

3.4.3 Brain Connectivity Analysis on Resting-State fMRI

We used CONN toolbox [134] to process rs-fMRI and 3D-T1 data, with SPM 12 and MATLAB R2021b (9.11) implementation. The steps of the processing pipeline included: 1) Functional realignment and motion assessment; 2) Slice-timing correction; 3) Outlier detection and head motion correction; 4) Normalization of functional and structural data to MNI space; 5) Data segmentation into gray matter, white matter and cerebrospinal fluid regions; 6) Functional smoothing with a full-width-half-maximum (FWHM) of 6 mm; 7) Denoising with linear regression and temporal band pass filtering between 0.01 and 0.1 Hz; 8) Detrending; 9) Parcellation of the gray-matter of co-registered anatomical and functional images into 136 regions of interest (ROI) based on the automated anatomical labeling – AAL atlas. All co-registered anatomical and functional images were inspected to ensure correct co-registration and anatomical parcellation. Finally, we extracted average timeseries from each ROI and constructed ROI-to-ROI connectivity matrices, representing the connectivity of every ROI to the remaining ones [134]. Specific ROI-to-ROI connectivity matrices were obtained for HGG, LGG and HC groups in the whole brain ROIs, left and right hemispheric ROIs. A graph theory analysis was performed starting from each ROI-to-ROI matrix with the Louvain Algorithm in CONN toolbox. For each patient a threshold of $z>2$ and $p<0.05$ was set to obtain the graph adjacency matrix from the respective ROI-to-ROI matrix. We computed graph-theoretical measures on the resulting graphs to address their topological properties [135]. Seven graph-theoretical metrics were calculated applying two-sided FDR correction ($p<0.05$): global/local efficiency (representing the global and local connectivity of each ROI), betweenness centrality (a measure of the tendency of a node to be part of the shortest path between any two pairs of nodes in a graph), average path length (shortest distance between the current node and all other nodes), clustering coefficient (ratio of connected nodes to all neighboring nodes), cost (proportion of edges

from a node), and degree (the number of nodes to which a selected node is connected) [135]. We used the above graph-theoretical metrics to evaluate the connectedness and integration of every node in the local and global network. We evaluated the small-worldness of the resulting graphs as the combination of elevated clustering coefficient - short average path length, as well as elevated global/local efficiency and low cost [135].

3.5 Structural Analysis through Voxel Based Morphometry (VBM)

In the following paragraphs we describe the structural analysis workflow related to SA#2. As detailed below, we employed voxel-based morphometry (VBM) to test the hypothesis that atypical dominance measured by fMRI lateralization (co- and right dominance) is associated with increased cortical volume of newly active cortices in the right hemisphere. Study groups and statistical comparisons are described in the statistics section (3.6).

For this specific aim, 3D T1-weighted anatomical images were processed with FSL-Voxel Based Morphometry (VBM) toolbox [136–138]. The analysis was focused on the right hemisphere only, due to signal loss and/or artifacts related to the presence of the tumor in the left hemisphere. The steps of the processing pipeline included: 1) 3D T1-weighted anatomical images were co-registered to the MNI 152 standard space through non-linear registration (ANTS); 2) The images were skull-stripped, the grey matter was segmented and the resulting images were averaged and flipped along the x-axis to create a left-right symmetric template; 3) Native grey matter images were non-linearly registered to the template and corrected for local expansion or contraction related to the non-linear spatial transformation; 3) The modulated grey matter images were smoothed with an isotropic Gaussian kernel with sigma = 3mm; 4) Cortical volume maps were generated with FSL randomize tool by applying voxel-wise t-test to identify significant voxels [139] (see statistical analysis). The location of the resulting clusters was confirmed on the Harvard-Oxford Cortical Structural Atlas and Harvard-Oxford Subcortical Structural Atlas [140].

3.6 Statistical Analyses

3.6.1 SA#1: To demonstrate language reorganization in brain tumors with fMRI and to identify tumor- and patient-related determinants of language plasticity

We created five binary variables corresponding to hemispheric LI, Broca's LI, Wernicke's LI, frontal LI, and temporal LI, with the cut-off of 0.2 [141]. Values of LI≥0.2 were defined "left-dominant" (LD, binary value = 1), while values <0.2 were defined "atypical dominant" (AD, binary value = 0), grouping co-dominant (-0.2<LI<0.2) and right-dominant subjects (LI<-0.2). The percentage of atypical dominant patients in our cohort was compared to the expected percentage in the healthy population, according to previous studies[70,71]. To identify patient and tumor features associated with language reorganization, we used the Chi-square test to study the relationship between LI variables and patient sex (0=female, 1=male), handedness (0=left, 1=right), tumor pathology (1=grade I/II, 2=grade III/IV, 3=metastasis), tumor location (frontal, parietal, temporal, occipital, insular, 0=involved/1=not involved), genetic and molecular data (IDH mutation, MGMT hypermethylation, EGFR amplification, FGFR mutation, 0=positive/0=negative). For those variables having significant Chi-square test results, contingency coefficient, phi factor, and Cramer's V were computed. Statistical analyses were performed on SPSS (Armonk, NY: IBM Corp. Version 25.0). We set the significance threshold for all analyses to $p<0.05$.

3.6.2 SA#2: To investigate anatomical changes of the cortex in patients with language reorganization by means of structural MRI techniques

Three VBM analyses were carried out in this objective, following the workflow described in section 3.5. First, the cortical volume of the right hemisphere of patients with atypical language dominance (co- or right dominant - AD) was compared to that of left dominant patients (LD). Subsequently, we separated patients in HGG and LGG sub-groups. The VBM analysis was repeated to compare AD patients and LD patients in each of these two sub-groups. Language dominance was calculated based on the hemispheric LI obtained in SA#1. As detailed in prior sections, differential cortical volume maps were generated with FSL by using non-parametric permutation testing corrected for multiple comparisons [139]. The minimum t-score=2 (corresponding to a $p<0.05$) was

applied as a threshold to identify significant voxels. To contain false positives, only clusters > 5 mm^3 were considered acceptable in the results [142,143]. Patients' age was compared through the Mann-Whitney U-test in the different groups ($p<0.05$). The statistical analysis was performed with SPSS Statistics (v.21, IBM, N.Y., USA) and FSL (FMRIB Software Library v5.0).

3.6.3 SA#3: To characterize different patterns of language reorganization in brain tumors by means of fMRI, graph theory and intra-operative stimulation

- Experiment 1

Starting from rs-fMRI data, we analyzed whole-brain and hemispheric functional networks in 30 patients with LGG, 30 patients with HGG, and 20 HC. Subsequently, we studied lobar networks in sub-groups of patients divided by tumor location. For every network we calculated the graph-theoretical measures explained in section 3.4.3 and compared the results in LGG vs. HC and HGG vs. HC through two-tailed Student t-test (in case of normal distribution) or Mann-Whitney U-test (in case of non-normal distribution) ($p<.05$). The Jarque-Bera test with chi-squared distribution and two degrees of freedom was used to confirm the normality of our data before statistical comparison [144]. The workflow of the study is summarized in Figure 4.

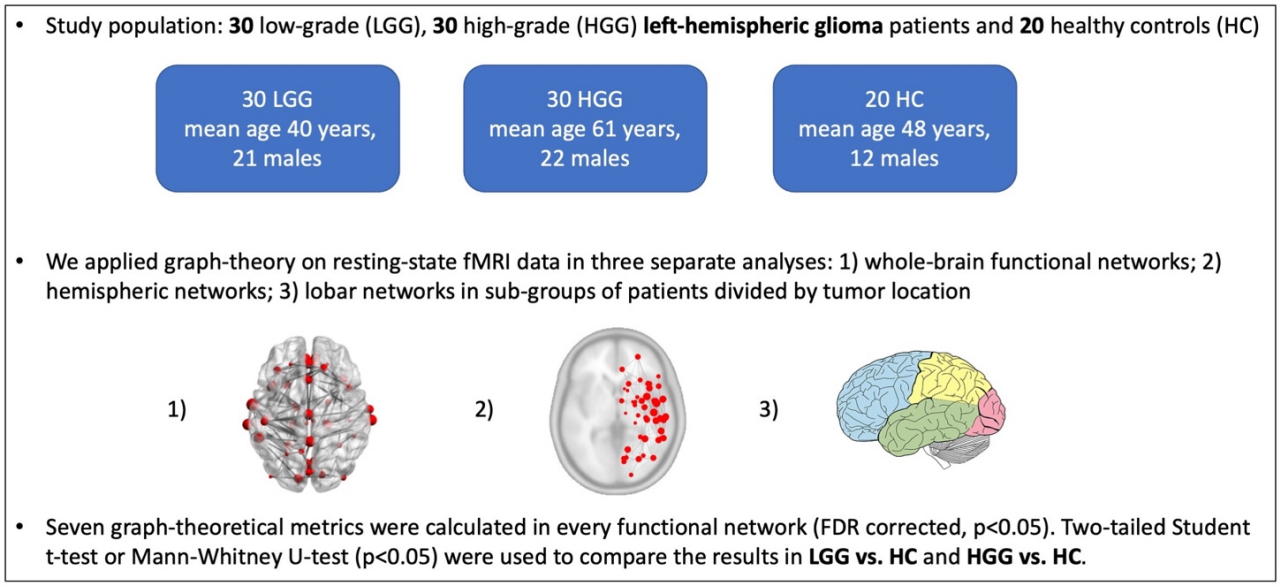

Figure 4. Workflow of SE#3, Experiment 1 (from [121])

The analysis on whole-brain, hemispheric and lobar networks was conducted with averaged graph-theoretical measures computed respectively on the whole brain, left and right hemispheres, and cerebral lobes (frontal, parietal, occipital, temporal, insular). For the lobar analysis, we divided patients based on lobar involvement from the tumor. Then, we selected the nodes belonging to the involved lobe from the graph and we analyzed them as a separate network. For example, nodes belonging to the frontal lobe were compared in patients with frontal lobe LGG and HGG vs. HC.

- Experiment 2

In a prospective cohort of 5 patients, we analyzed individual functional language networks prior to tumor resection (baseline) and at three intervals after surgery: post-op1 (4-8months), post-op2 (10-14months), post-op3 (16-23months), through longitudinal fMRI, graph theory and language clinical assessment. Functional correlation maps were generated at minimum threshold of $r>0.5$ (uncorrected $p=2x10^{-11}$, $t>4$, FDR-adjusted p value<0.001) from tb-fMRI, and used for conjunction analysis. Individual language networks were obtained using functional ROIs and optimal percolation thresholding, as described in section 3.4.2. We established language dominance on tb-fMRI as described in section 3.4.1, focusing on Broca's LI for the purpose of this experiment. The connectivity of individual language networks was quantified through a 'Connectivity laterality Index' (CI), as described in section 3.4.1. We assessed the trend of the intra-patient correlation of LI and CI values at the four time points with a linear mixed model (LMM) or linear model, when no cluster effects were detected. Correlation between language performance and LI/CI was also evaluated with the same model. Statistical significance threshold was set at $p<0.05$.

- Experiment 3

In a selected group of patients who underwent awake surgery with intra-operative stimulation of dominant language cortices (inclusion criteria in section 3.1), we compared functional language networks of those with speech arrest (SA) vs. those without speech arrest (NSA). Individual language networks were obtained using functional ROIs from Task-based fMRI maps by applying optimal percolation thresholding, as in Experiment 2 (method described in section 3.4.2). The connectivity of individual language networks was quantified through a 'Connectivity laterality Index' (CI), as in

Experiment 2 (method described in section 3.4.1). The CI of SA and NSA patients was compared through the Mann-Whitney U-test ($p<0.05$).

We also tested the association between speech arrest and tumor-related variables as detailed below. We created a binary variable corresponding to speech arrest (0 = NSA, 1 = SA), and 10 binary variables corresponding to: pre-operative speech deficits (0=absent, 1=present), post-operative speech deficits (0=absent, 1=present), speech deficits at 3-6 months (0=absent, 1=present), prior surgery (0=absent, 1=present), handedness (0=left, 1=right), frontal tumor location (0=not involved, 1= involved), temporal tumor location (0=not involved, 1= involved), insular tumor location (0=not involved, 1= involved), invasion of BA (0=not involved, 1= involved), invasion of WA (0=not involved, 1= involved). Chi-squared test was employed to identify the relationship between speech arrest and other nominal variables. For those variables having significant Chi-square test results, contingency coefficient, phi factor, and Cramer's V were computed. The analysis was repeated for significant variables in subgroups of patients divided by tumor grade. Statistical analyses were performed on SPSS (Armonk, NY: IBM Corp. Version 25.0). We set the significance threshold for all analyses to $p<0.05$.

4 RESULTS

4.1 SA#1: To demonstrate language reorganization in brain tumors with fMRI and to identify tumor- and patient-related determinants of language plasticity

Four hundred and five patients were recruited for this objective. One hundred and six patients were diagnosed with low-grade glioma (LGG, WHO grade 1–2); 242 patients were diagnosed with high-grade glioma (HGG, WHO grade 3–4); and 57 patients were diagnosed with metastatic disease. Due to retrospective design, molecular features were only available for part of the subjects. IDH status was present in 240/405 patients (124 wild-type); MGMT status in 255/405 (144 unmethylated); EGFR in 188/405 (46 amplified); FGFR in 198/405 (16 mutated). The age distribution of AL and LL patients according to the calculated LIs was not significantly different on Mann-Whitney U test.

	HGG	LGG	METS
Age (mean and SD)	53 +/- 14	43 +/- 13	54 +/- 13
Sex	152M; 90F	56M; 50F	27M; 30F
Handedness	216R; 26L	92R; 14L	53R; 4L
Frontal lobe	126	59	37
Temporal lobe	88	40	12
Parietal lobe	65	14	18
Occipital lobe	8	2	2
Insula	45	36	1
BA	54	21	2
EA	28	19	3
SMA	30	12	8
WA	30	5	5
SMG	16	3	6
AG	18	3	4

Language lateralization based on hemispheric LI demonstrated 210 LL and 195 AL patients. Frontal LI demonstrated 221 LL and 184 AL patients. Broca's LI demonstrated 234 LL and 171 AL patients. Temporal LI demonstrated 220 LL and 185 AL patients. Wernicke's LI demonstrated 215 LL and 190 AL patients. Laterality results are summarized in Figure 5.

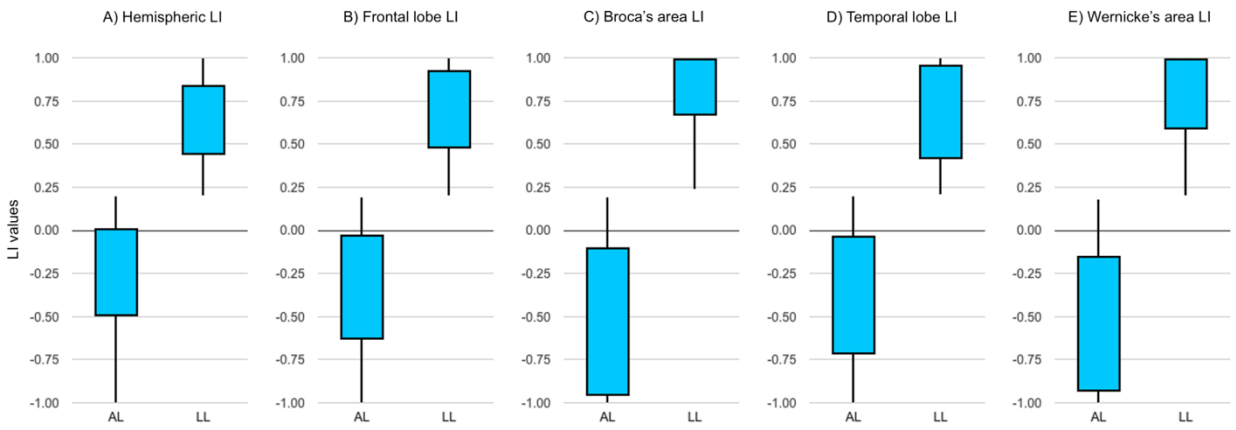

Figure 5. Laterality distribution according to the 5 calculated LI in the tumor population

The Chi-square analysis for tumor location demonstrated a significant correlation between atypical dominance and tumor involvement of BA (Chi-square p<0.001; Fisher p<0.001). None of the remaining locations produced significant results. The Chi-square analysis for genetic and molecular data demonstrated a significant correlation between higher grades and atypical dominance (Chi-square p<0.001; Fisher p<0.001). EGFR amplification was significantly associate with atypical dominance (Chi-square p=0.042; Fisher p=0.05). FGFR mutation correlated significantly with left dominance (Chi-square p=0.019; Fisher p=0.021). In HGG only, MGMT hypermethylation correlated with language reorganization (Chi-square p=0.016; Fisher p=0.014). Finally, female sex was significantly associated with AL (Chi-square p=0.005; Fisher p=0.001), while patients' handedness did not show any significant correlations.

4.2 SA#2: To investigate anatomical changes of the cortex in patients with language reorganization by means of structural MRI techniques

One-hundred nineteen patients were recruited for this objective (mean age 50 years, range 22-80 years, 77 males), 44 with LGG (WHO 2016 grade 2, mean age 47 years, range 22-68 years, 27 males) and 75 with HGG (WHO 2016 grade 3 and 4, mean age 53 years, range 23-80 years, 43 males). The vast majority of the subjects was right-handed (104/119). Age distribution was not significantly different between the study groups. Language laterality from tb-fMRI demonstrated

64/119 atypical dominant patients (AD, 56 right-handed, 8 left-handed) and 55/119 left dominants (LD, 48 right-handed, 7 left-handed). In LGG and HGG sub-groups, AD cases were 43% and 60% respectively.

In the first VBM analysis, we compared AD vs. LD patients (regardless of tumor grade). The analysis demonstrated increased cortical volume in AD patients in the following areas: right IFG, right STG, right insula, right fusiform gyrus, right precentral gyrus (preCG), right temporal-parietal junction (TPJ), right posterior cingulate cortex (PCC), right hippocampus, right and left lateral cerebellum. In the second VBM analysis, we compared AD vs. LD patients with HGG. This analysis showed increased cortical volume in AD patients in the following areas: right IFG, right STG, right insula, right fusiform gyrus, right preCG, right TPJ, right PCC, right hippocampus, right and left lateral cerebellum. In the last VBM analysis we compared AD vs. LD patients with LGG. We found increased cortical volume in AD patients in the following areas: right IFG, right STG, right insula, right fusiform gyrus, right anterior cingulate cortex (ACC), right PCC, right DLPFC. Selected language-related areas with increased cortical volume in AD patients are shown in Figure 6 and 7.

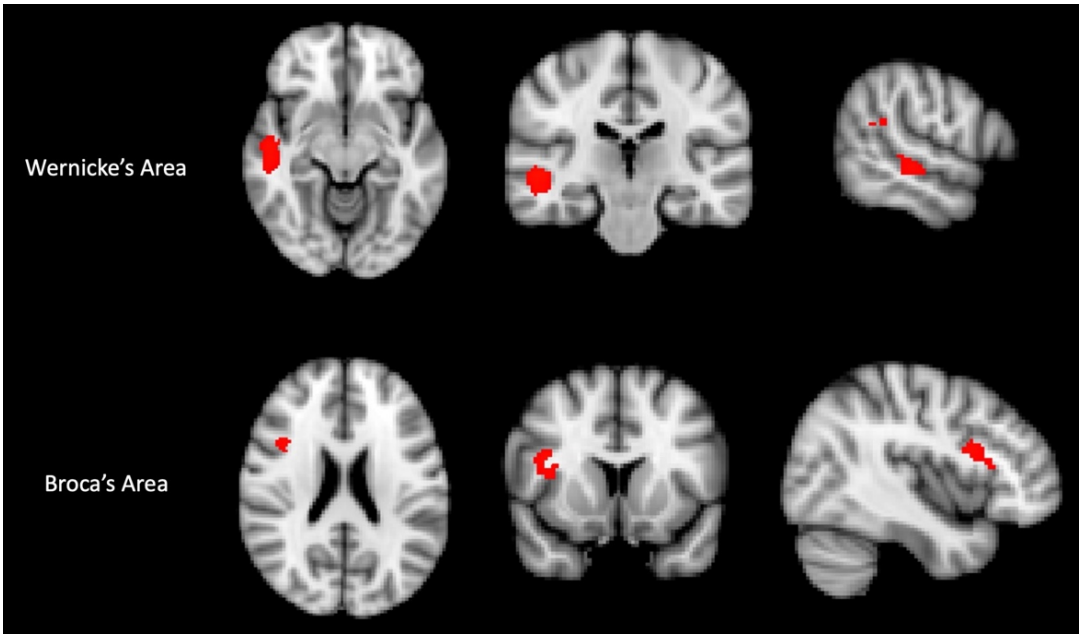

Figure 6. Atypical Dominant patients showed increased cortical volume in right-sided Wernicke's and Broca's area homologues

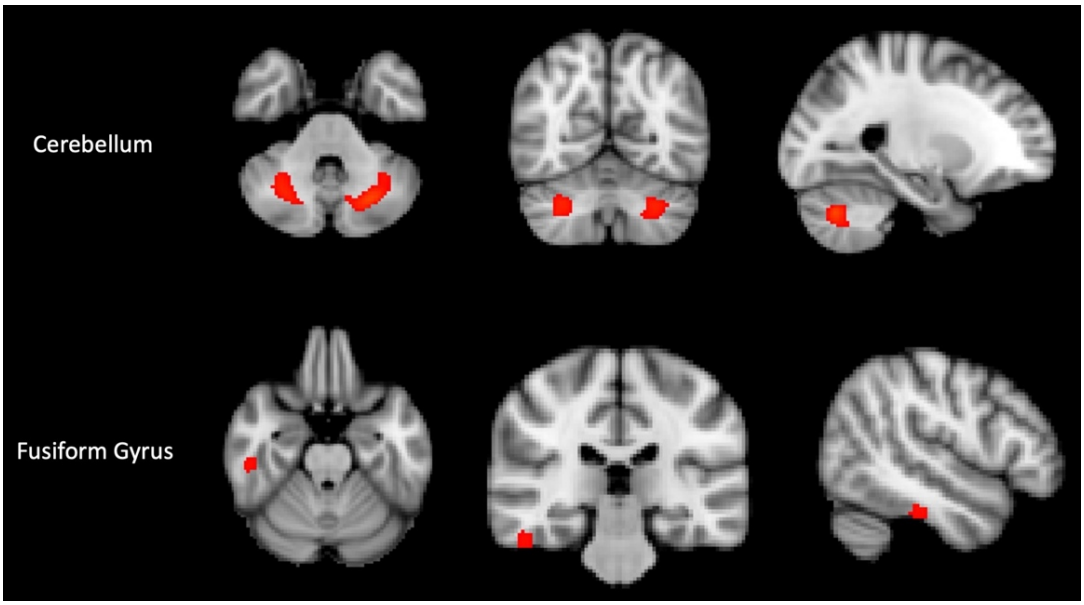

Figure 7. Atypical Dominant patients showed increased cortical volume in right-sided fusiform gyrus and bilateral cerebellum VI

4.3 SA#3: To characterize different patterns of language reorganization in brain tumors by means of fMRI, graph theory and intra-operative stimulation

4.3.1 Experiment 1: Analysis of whole-brain, hemispheric and lobar functional networks in 30 patients with LGG, 30 patients with HGG, and 20 HC

Graph Theory Analysis: Whole-brain and Hemispheric Network Analysis

The left hemispheric network of LGG demonstrated significantly increased global efficiency vs. HC ($p=0.03$). HGG displayed decreased cost and degree of the right hemispheric network compared to HC ($p=0.028$ and $p=0.028$ respectively). These findings are shown in Figure 8.

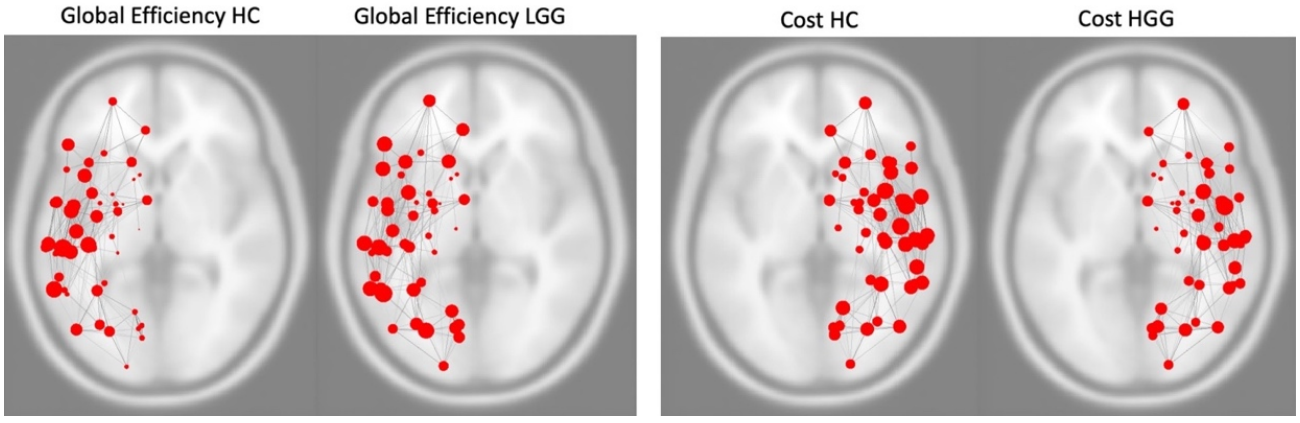

Figure 8. Graph-theory metrics in LGG and HGG hemispheric networks compared to HC

LGG showed significant differences in left vs right hemispheric network (increased global efficiency p=0.02; decreased local efficiency p=0.01 and clustering coefficient p=0.01). No significant differences emerged from the comparison of hemispheric networks in HGG and HC, as well as whole-brain networks.

Graph Theory Analysis: Lobar Networks Analysis

Frontal tumors showed significant network changes in many areas of the left and right hemisphere regardless of tumor grade. Right-sided changes were located in the Superior Frontal Gyrus (SFG), while left-sided changes involved the SFG, MFG, and IFG pars triangularis. Temporal tumors displayed right-sided changes in the STG posterior division, MTG posterior division, MTG temporo-occipital part, and ITG anterior division. Left-sided changes were located in STG anterior division, STG posterior division, MTG anterior division, and ITG anterior division. In parietal and insular tumors, network modifications were limited to left hemisphere: parietal tumors demonstrated network changes the left Postcentral Gyrus and left AG; Insular LGG were associated to local changes, while HGG did not produce any significant effects.

4.3.2 Experiment 2: Analysis of individual functional language networks prior to tumor resection (baseline) and at three intervals after surgery in a prospective cohort of 5 patients with LGG

The cohort of patients analyzed with longitudinal tb-fMRI and graph-theory included 5 100% right-handed subjects (4 males, mean age 47.6 years) with left-hemispheric LGG involving the frontal and/or temporal lobe, in the region of eloquent language areas. These patients underwent 4 fMRI scans with the same phonemic fluency task at the following intervals: pre-op (baseline), post-op1 (4-8months), post-op2 (10-14months), post-op3 (16-23months).

Visual inspection of fMRI maps demonstrated initial left dominance in 3/5 patients and bilateral activation in 2/5 patients. Over time, increased right-sided activation was noted in the cases originally displaying left-dominance (Figure 9).

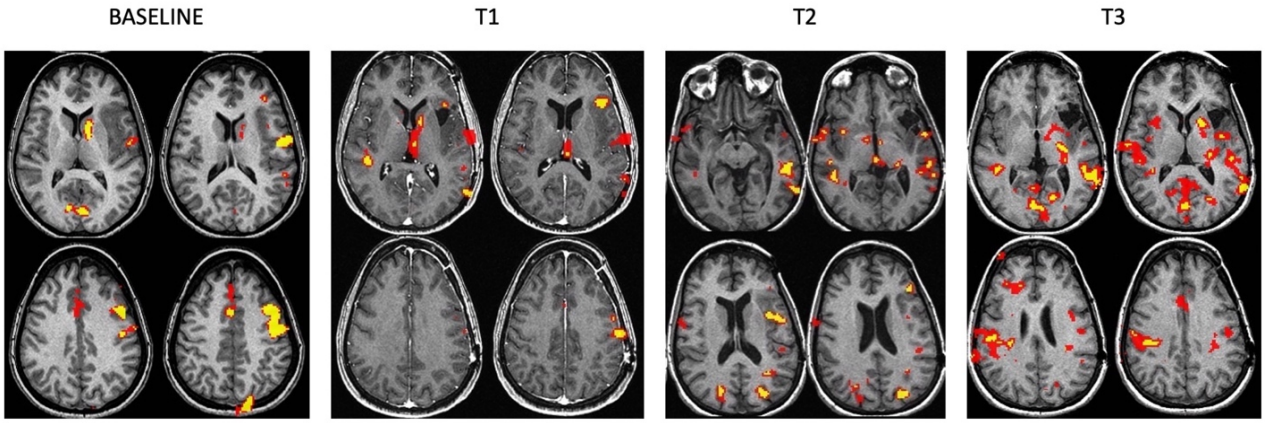

Figure 9. Representative case for Type 1 language reorganization. The images show fMRI activation maps obtained with letter task. The patient was left-dominant on the preoperative fMRI (baseline), with strong activation of Broca's area. After surgery, a progressive increase of right-side activations emerges from fMRI maps. T1=4-8 months, T2=10-14 months, T3=16-23 months.

The 2 patients showing more-than-expected right-sided language activation at baseline maintained a state of co-dominance up to the last post-operative timepoint (Figure 10).

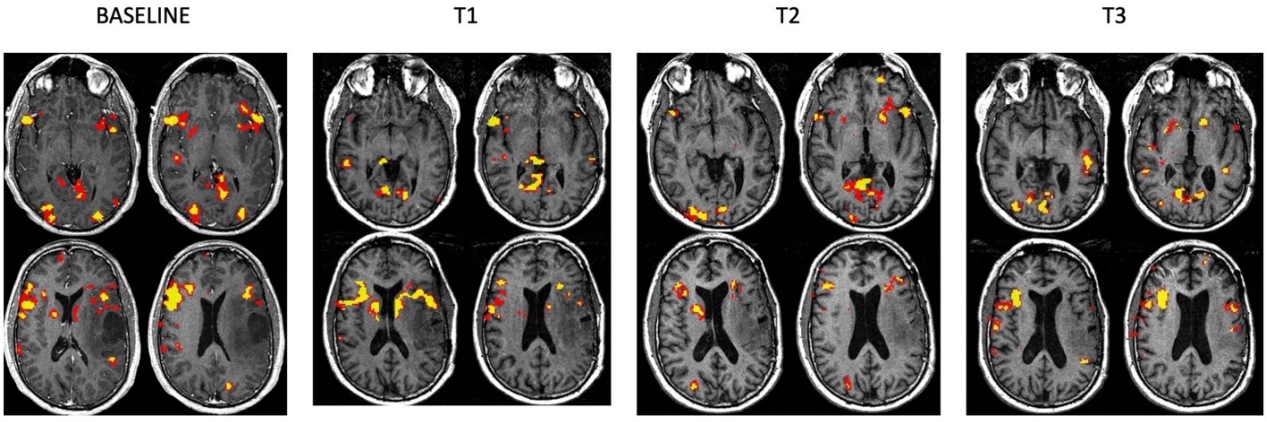

Figure 10. Representative case for Type 2 language reorganization. The images show fMRI activation maps obtained with letter task. The patient was co-dominant on the preoperative fMRI (baseline), with strong activation of right-sided Broca's area homolog. After surgery, atypical dominance is maintained throughout the follow-up period. T1=4-8 months, T2=10-14 months, T3=16-23 months.

The Broca's LI calculated on fMRI maps confirmed the findings observed at visual inspection (Figure 11). The linear mixed model used to compare LI values across each patient's timepoints

demonstrated a significant decreasing trend ($p < 0.001$). No significant correlation was found between LI values and language performance (BNT $p=0.19$, PVF $p=0.64$, CF $p=0.21$).

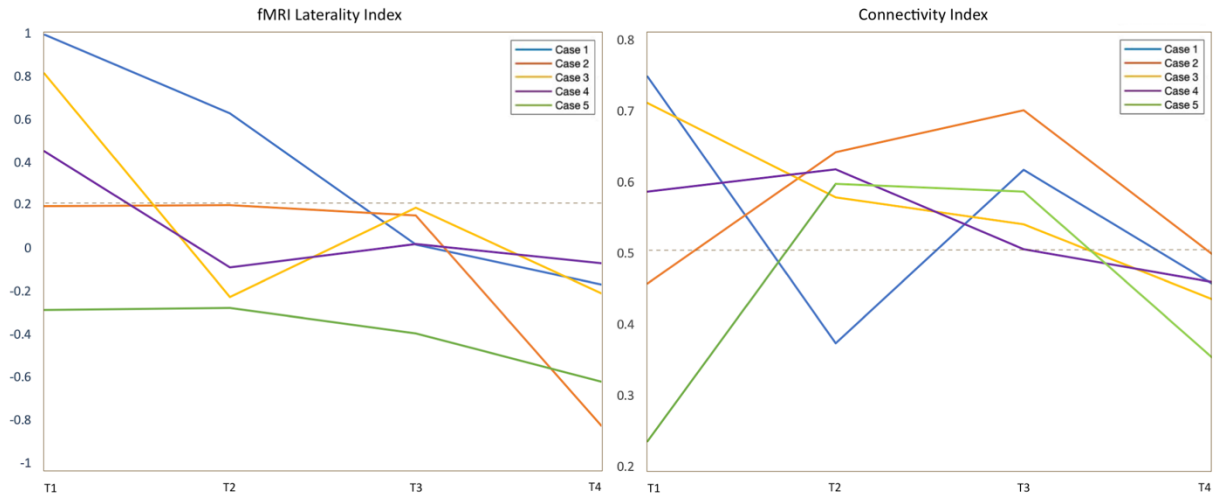

Figure 11. The left panel shows the fMRI laterality index for all cases across the four timepoints of the study (T1-T4). Values above 0.2 were considered left dominant. The right panel shows the connectivity laterality index for all cases across the four timepoints of the study (T1-T4). The closer the values are to 0.5, the more balanced is the connectivity between the two hemispheres. Values above 0.5 point to higher participation of the left hemisphere. (Submitted for publication)

Connectivity diagrams obtained through optimal percolation technique provided a similar picture to that of fMRI maps: 3/5 patients showed predominant left hemispheric connections at baseline (Figure 12), while bilateral connectivity was noted in 2/5 patients (Figure 13). Over time, the cases originally displaying left-dominance showed a progressive increase in right-sided inter-hemispheric connections, including language-related areas: BA (5/5), WA (3/5), premotor cortex (2/5), middle frontal gyrus (5/5), insula (3/5).

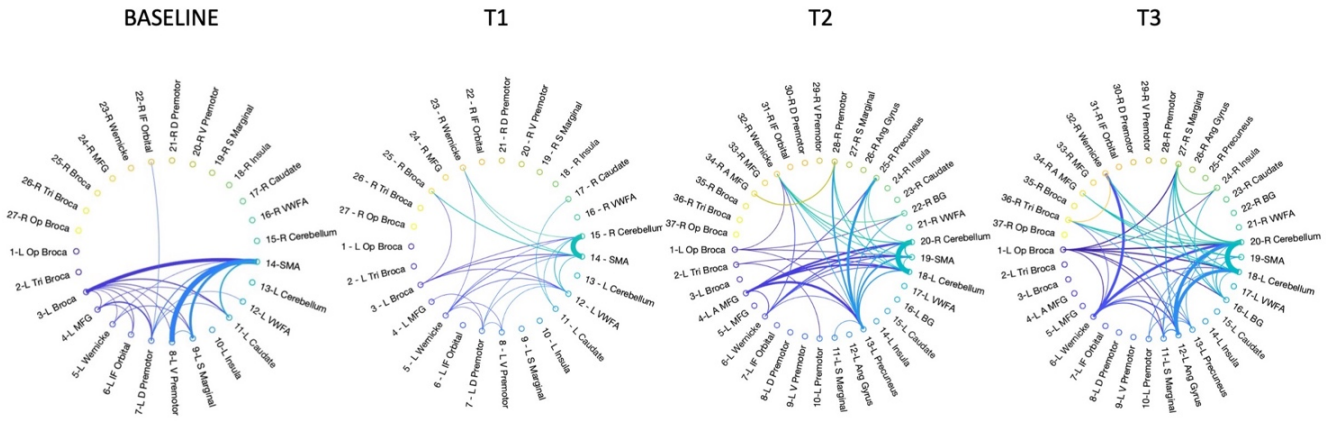

Figure 12. Representative case for Type 1 language reorganization. The images show connectograms obtained with optimal percolation theory. The patient showed predominant left connectivity on the preoperative timepoint (baseline). After surgery, a progressive increase of right-side connectivity emerges from the diagrams. T1=4-8 months, T2=10-14 months, T3=16-23 months.

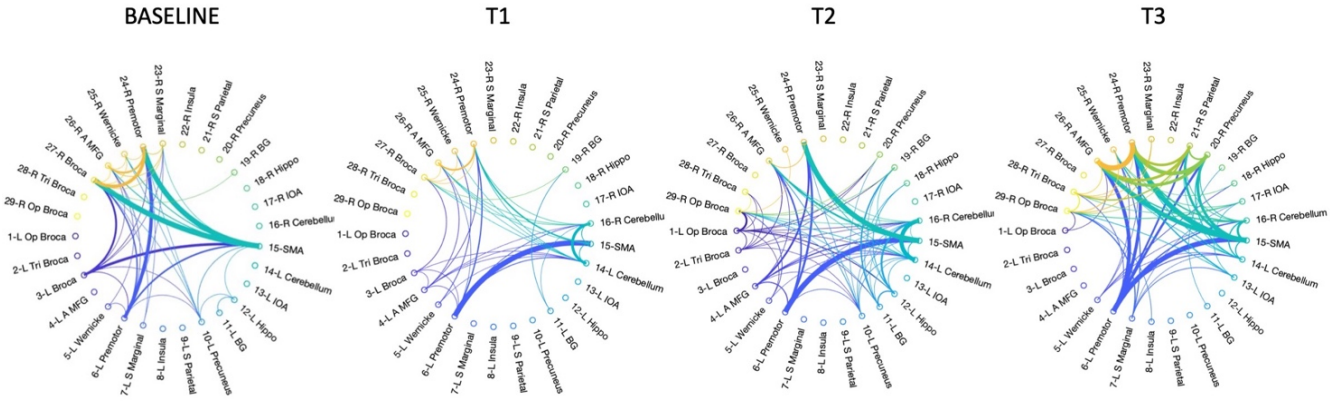

Figure 13. Representative case for Type 2 language reorganization. The images show connectograms obtained with optimal percolation theory. The patient showed bilateral connectivity on the preoperative fMRI (baseline). After surgery, bihemispheric connectivity is maintained throughout the follow-up period. T1=4-8 months, T2=10-14 months, T3=16-23 months.

The CI evaluation confirmed these results, by showing predominant left hemispheric connectivity at baseline in the same 3/5 cases and more bilateral connectivity in the remaining 2/5 patients (Figure 11). In particular, case 1 changed from 0.75 to 0.46 on the last follow-up; case 3 shifted from 0.71 to 0.44; case 4 changed from 0.59 to 0.46**.** Two/five cases maintained high bihemispheric connections throughout the scans: the CI of case 2 changed from 0.46 to 0.50 on

post-op 3; case 5 shifted from 0.24 initially to 0.35 on post-op 3 (0.5 representing perfectly balanced connections between the hemispheres). However, the statistical analysis of CI values did not confirm a significant decreasing trend (p=0.27), probably due to initial fluctuations at the first post-surgical timepoint. No significant correlation was found between CI values and language performance (BNT p=0.29, PVF p=0.97, CF p=0.11).

4.3.3 Experiment 3: Comparison of functional language networks in patients with speech arrest (SA) vs. no speech arrest (NSA) during intra-operative cortical stimulation.

The patients recruited for this experiment included 44 subjects (28 males, mean age 44.4 years) with left perisylvian LGG.). Tumors involved the frontal lobe (29), insula (19) and temporal lobe (9). BA was involved by 17 tumors, Wernicke's area (WA) by 4 tumors. Twenty-four patients demonstrated speech arrest during awake surgery, while 20 showed no speech arrest.

Connectivity diagrams obtained through optimal percolation technique showed increased total number of intra- and inter-hemispheric links in NSA patients. Besides increased whole-brain connectivity, the diagrams showed enhanced right-sided connections intra- and inter-hemispheres across scans, including language-related areas (Figure 14).

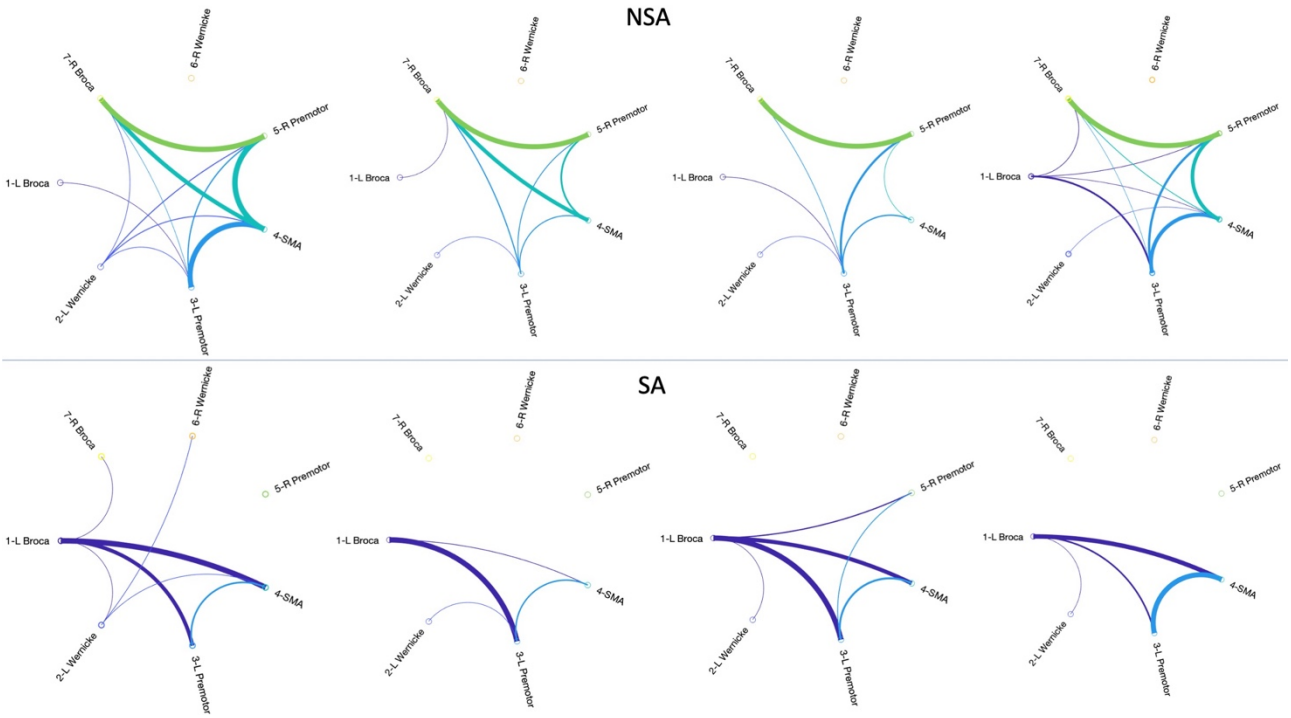

Figure 14. Representative cases for patients with speech arrest (SA) and no speech arrest (NSA) during intra-operative stimulation of left dominant language areas. The images show connectograms obtained with optimal percolation theory. Patients with SA showed left localization of core language areas. In NSA patients, the language network was more bilateral, with increased recruitment of the right hemisphere

The CI evaluation demonstrated increased connectivity of right-sided core language areas in NSA compared to SA patients, as demonstrated by the Mann-Whitney U-test ($p<0.001$). The mean CI for NSA patients was 0.48, with standard deviation of 0.2. The mean CI for SA patients was 0.80, with standard deviation of 0.09.

The Chi-square test identified significant correlations between speech arrest and the following variables: Pre-operative speech deficits ($p=0.011$, more in SA), post-operative speech deficits ($p=0.006$, more in SA), insular tumor location ($p=0.017$, more in NSA), Broca's area invasion ($p=0.023$, more in NSA).

5 DISCUSSION

5.1 Tumor growth in the left hemisphere is associated with inter-hemispheric language reorganization and structural modifications of cortical volume

Our results confirmed that patients with left-hemispheric tumors develop more right-hemispheric activation than what is expected in the normal population from prior studies (Figure 5) [70,71]. Such findings support the idea of tumor-induced language plasticity. Furthermore, we demonstrated that inter-hemispheric language reorganization in patients harboring left-hemispheric gliomas is associated with increased cortical volume in right-sided language-related areas. These areas include BA homolog, WA homolog, the right fusiform gyrus (involved in face-recognition and semantic processing [40]) (Figure 6 and 7). Cortical volume increases were also detected in the left and right lateral cerebellum (segment VI), which is known to host language function [46] (Figure 7). The reorganization of cerebellar networks in patients with brain tumors has already been shown in previous studies [88], including the association with increased cortical volume [89]. These results

support the idea that tumor growth in the left hemisphere determines contralateral reorganization of the language network, characterized by new cortical activations and underlying increase in cortical volume.

Modifications of cortical volume in language reorganization may depend on different mechanisms. Synapse formation and cortical rewiring may be promoted by neuronal activity and transmitter release in intensely activated areas [58]. Draganski at al. demonstrated that the process of learning new functions may lead to cortical thickening of specific brain areas involved in the improved function [61]. For example, exercising may lead to increased volume of the motor cortex in mice [145]. Such modification can develop as soon as after three to six months of training in humans [62,116]. In a similar way, brain lesions may induce synaptogenesis and rewiring, even from afar. Dancause et al. studied the effects of ischemia on the brain of squirrel monkeys, demonstrating extensive perilesional axonal sprouting, with the formation of new connections with distant regions [69]. Based on our results and previous literature, we theorize that patients with left-hemispheric brain tumors invading eloquent language areas can recruit contralateral homologues, leading to intense activation of these areas and increased cortical volume (Figure 15).

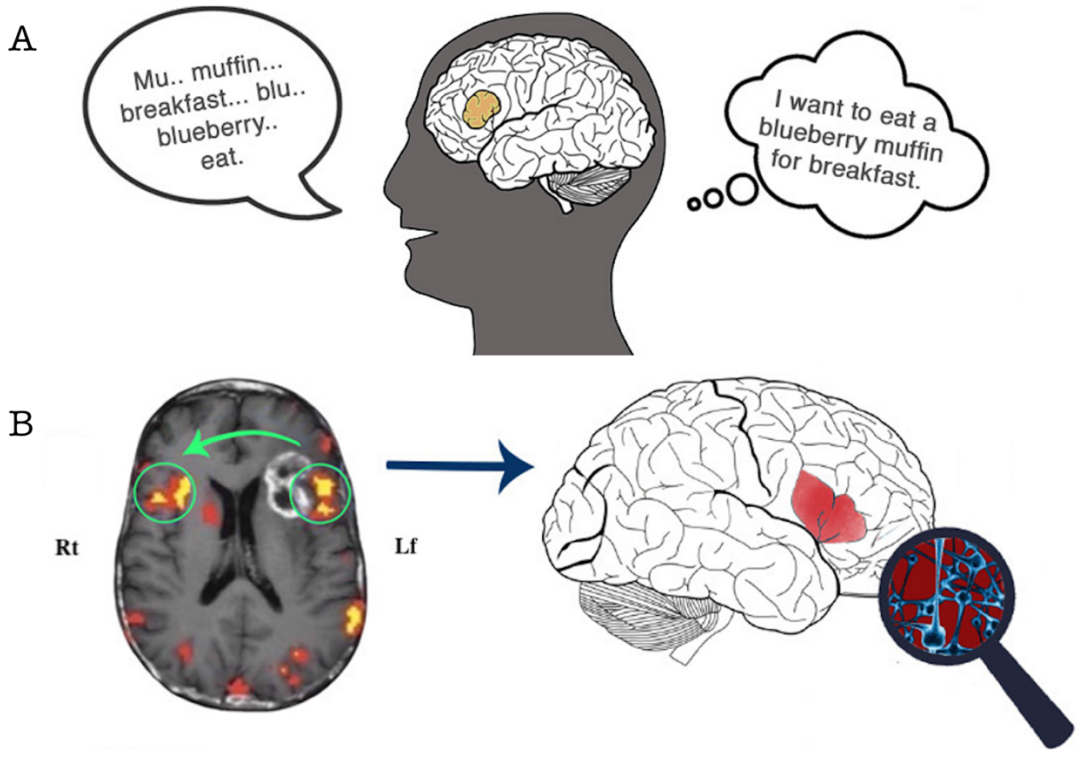

Figure 15. Exemplification of our theory regarding the neurobiology of language reorganization. The brain recruits language areas homologues in the right hemisphere to overcome clinical deficits (A). The intense activation of newly recruited areas leads to synaptogenesis and increased cortical volume (B).

5.2 Language reorganization appears to be influenced by age, sex, frontal location, BA and WA invasion, tumor pathology, EGFR amplification, IDH mutation, MGMT methylation, FGFR mutation

Currently, there is poor understanding of the determinants of language plasticity, meaning tumor and patient features which are associated with increased likelihood of reorganization. Specific tumor locations associated with plastic phenomena have seldom been investigated before [27,80]. We found a significant correlation between atypical dominance on frontal and Broca's LI, and involvement of BA from HGG. Prior evidence from IOS during awake surgery suggests that BA may be more prone to plasticity than other eloquent language areas, with the potential of reorganizing to surrounding frontal or insular cortices [15]. As a consequence, brain tumors invading frontal areas may more often produce in cortical reorganization than those in temporal regions [80]. Our results are in agreement with these findings, confirming BA propensity for plasticity in the form of inter-hemispheric reorganization.

Tumor genetic and molecular features demonstrated a significant correlation with language laterality. These features influence the tumoral cytoarchitecture, guide tumor growth, pattern of spread, and interaction with its surroundings. In our results, MGMT hypermethylated HGG demonstrated increased language reorganization. This fact can be explained by the survival advantage of such epigenetic change [146], with the result of more time to develop plasticity. Increased right-hemispheric activity was also associated with EGFR amplification, which is known to affect tumor vascularity and perfusion [147,148]. The result can be at least partially explained with the correlation between increased tumor vascularization and neuro-vascular uncoupling (NVU) [149], which implies the suppression of peritumoral BOLD signal ("pseudo-reorganization"). Language reorganization was also associated with lack of FGFR mutations. FGFR abnormalities are oncogenic by promoting tumor proliferation and migration [150], and they are frequent in

glioblastomas [150]. Consequently, increased proliferation and tumor aggressivity related to FGFR mutation may limit the plastic potential of the brain.

5.3 Tumors of different location produce different effects on brain connectivity, both locally and in distant regions. LGG may show more favorable connectivity changes than HGG

We found increased global efficiency of the left hemispheric network in LGG patients (ipsilateral to the tumor) compared to HC (Figure 8), which points to higher inter-connectedness and more efficient information transfer. Other authors described similar increments of brain connectivity in glioma patients compared to healthy subjects. These network modifications may represent intra-hemispheric reorganization in the setting of LGG, a widely described phenomenon [15,98]. The novelty of our results consists in the evaluation of the reorganized network through graph-theory metrics, which demonstrated beneficial changes in terms of network efficiency. Our results point to a higher inter-connectedness of the entire left-hemispheric network in LGG, with decreased locality (sub-graphs are less inter-connected within their neighborhood and more connected to the entire network). These changes suggest a type of functional reorganization centered on the expansion of the left hemispheric network by recruitment of ipsilateral brain regions and shift from locality to global efficiency.

The situation was different in HGG, with a trend of decrease in all graph metrics values in the left hemisphere compared to HC, although without reaching statistical significance. Peritumoral BOLD signal depression is expected in HGG due to NVU [151,152], which translates into local connectivity impairment [153]. On the other hand, the hemispheric connectivity analysis in HGG showed significant decrease of cost and degree in the right hemispheric network compared to HC (Figure 8). Many studies support the idea of gliomas producing global effects on the brain, including alterations of the function of remote areas [154]. These tumors are deemed to involve the 'whole-brain' through widespread microscopical infiltration since early stages [155]. The decreased cost and degree of the right hemispheric network seem to highlight the specific effect of HGG on brain connectivity. Aggressive tumors may reproduce the effects of a stroke, including the phenomenon

of diaschisis, described as loss of excitability, reduced metabolism and/or blood flow in remote areas with respect to the causative lesion [156]. Diaschisis can lead functional changes of the brain connectome, including disconnection and reorganization of distant sub-graphs [156]. Our results seem to support a similar effect on functional connectivity driven by the rapid growth of HGG. Our findings also point to a certain degree of inter-hemispheric reorganization in HGG, as described by prior studies, including translocation of eloquent language areas[7,8,79].

The analysis of lobar networks further highlighted the importance of tumor location for network changes. Frontal and temporal tumors showed bihemispheric modifications of functional connectivity, while parietal and insular tumors demonstrated local effects only (i.e. limited to the left hemisphere). This may be related to higher concentration of eloquent cortices in the left frontal and temporal lobes [47], compared to parietal and insular cortices [157]. Eloquent areas may act as 'connectors' in the functional connectome [77], leading to deeper modifications of the network when damaged from a tumor compared to peripheral areas [158]. Additionally, functional modifications induced by temporal tumors consisted in the decrease of all graph metrics in both hemispheres, regardless of tumor grade. Briganti et al. investigated the effects of posterior vs. anterior tumors on the connectivity of the language network, showing decreased functional connectivity in posterior gliomas [74]. Based on these findings, we may speculate that temporal tumors exert detrimental effects on brain connectivity, while plastic changes may more likely occur with frontal lesions.

5.4 Two patterns of language reorganization were identified: Type1 changes may in part be treatment-related; Type2 may be tumor-induced, since already present at baseline

Language reorganization across the cerebral hemispheres in LGG patients may reflect different factors. Through serial fMRI acquisitions we were able to observe the development of plastic changes over more than 12 months, making possible to infer different patterns of reorganization. In Type 1 changes (Figure 9 and 12), patients showed strong left-dominance at baseline, with subsequent slow recruitment of the right hemisphere over the observation period. This type of plasticity appears to be influenced by the treatments which the patients were subject to, including

surgical resection. Previous authors provided strong evidence that surgical resection of brain tumors in eloquent language areas may be induce reorganization, possibly affecting the surgical outcome [98,100,159]. Other treatments may also play a role in this type of plasticity. Chemotherapy causes structural and functional modifications in the brain [160], which may persist after the recovery of cognitive deficits, suggesting that brain plasticity is tightly connected to functional recovery [160]. Our results support the use of longitudinal fMRI after surgery to monitor the development of reorganization and to tailor therapeutic interventions on a case-by-case basis.

Type 2 plasticity appears to reflect tumor-induced other than treatment-induced reorganization, because of their presence from the first scan, which was acquired pre-operatively (Figure 10 and 13). Tumor-induced language reorganization has been described by several prior studies, including inter- and intra-hemispheric modifications [7,8,14,97]. For example, Rosenberg et al. described inter-hemispheric translocation of BA over two years of observation before surgery in a patient with LGG [113]. Type 2 cases showed a relatively stable bihemispheric connectivity, with less visible left-to-right shift of activation than Type 1 patients. This fact may be related to different time-windows for the two types of reorganization, with surgery-induced functional changes being faster than tumor-induced plasticity. Patients with Type 2 plasticity also displayed larger tumors than Type 1, possibly indicating longer disease duration.

None of the 5 patients included in this analysis showed significant changes in language performance scores during the follow up period. This evidence may support the idea that inter-hemispheric language reorganization is not associated ‘per se’ with clinical improvement, as suggested by other authors [98]. Increased connectivity and recruitment of the right hemisphere may represent the initial step of reorganization, creating a permissive environment to develop compensatory phenomena [67]. On the other hand, the increased whole-brain connectivity and the right shift of activation may contribute to preserve language function against the negative effects of glioma invasion, surgical resection and chemo-radiation. Particularly, systemic treatments and brain radiation may determine inflammation and demyelination of the neural tissue, reduction of neurogenesis, and hormonal changes [160]. These factors can cause cognitive impairment and

affect brain connectivity [161,162]. In this view, plastic phenomena could at least partially compensate for treatments cognitive side effects, preventing further decline in performance [160].

5.5 Patients with lack of speech arrest during intra-operative stimulation displayed increased core connections in the right hemisphere and better clinical performance compared to patients with SA who retained the language core in the left hemisphere

The last experiment of this project explored the relationship between language reorganization observed intra-operatively during awake surgery and fMRI. We demonstrated the right-shift of language core connections on fMRI in patients with surgically-proven language reorganization (NSA) (Figure 14). Based on these findings, one may hypothesize the lack of speech arrest during IOS being associated with the development of new connections in the right hemisphere. Our results are in line with this hypothesis, showing significantly increased activity of right-hemispheric language areas homologues in NSA patients. Li et al. used fMRI and graph-theory to demonstrate the adaptive connectivity underlying language plasticity in a patient undergoing surgical resection of BA, showing the development of new connections: after surgery, the newly active right-sided BA homolog was connected to the remaining language areas through the SMA [14]. In the current study, patients with reorganized language showed connections with the right hemisphere that were not present in the healthy population nor in SA patients (Figure 14). These difference may point to the development of new connections in NSA patients, in a similar way to the study by Li et al. [14].

The other main result of this experiment was the evidence of improved clinical performance in patients with lack of speech deficits during IOS and right translocation of core language connections on fMRI. There are few reports about the clinical meaning of language reorganization. Rivera-Rivera et al. employed TMS to stimulate right-sided language areas prior to surgery, achieving low postoperative deficits despite resection of eloquent cortex [163]. Shaw et al. reported that patients with language reorganization may show better performance on the BNT [42]. In a similar way, Quinones et al. associated the longitudinal development of reorganization with decreased post-treatment aphasia [164]. In our study, we evaluated the presence of speech deficits at three

timepoints via standard neurologic testing. We found significantly lower speech deficits in NSA patients at the time of surgery and in the immediate post operative setting, compared to SA patients. Conversely, differences in speech deficits 3 months after surgery were not statistically significant. This evidence supports the hypothesis of compensatory nature of inter-hemispheric language reorganization. In this view, right-sided language areas homologues take over the function of tumor-invaded cortices in the dominant hemisphere, leading to compensation of speech deficits. Compensatory (adaptive) plasticity has been described from a network perspective by previous authors. Deverdun et al. showed that the resection of brain tumors may lead to translocation of function to nearby areas [99]. Similar results have been reproduced in stroke [165]. In our patients, the better clinical performance before and immediately after surgery seem to suggest compensatory effects of tumor-induced plastic changes. If confirmed by future studies, the evidence of language reorganization may support clinical decision making in the preoperative setting, affecting the surgical approach and supporting a more aggressive tumor resection. Given time, the brain seem to actuate compensatory mechanisms even in patients who retained left lateralized language prior to surgery. In fact, speech deficits were similarly low in both patient groups 3-6 months after surgery. Although this experiment did not include post-surgical scans, we may speculate that SA patients developed some degree of language reorganization after surgery, similarly to the results of experiment 2 (Type 1 plasticity).

6 CONCLUSIONS

The discovery of new treatments has increased the life expectancy of patients with brain tumors, so that long-term life quality preservation has become pivotal in neuro-oncology. Language plasticity has direct effects on the clinical management of brain tumor patients, including surgical approaches and timing. Multi-step tumor resection has been proposed by Duffau et al. for LGG based on the fact that post-surgical development of plasticity may allow for better compensation of clinical deficits [166,167]. Furthermore, a better understanding of brain plasticity may enable the induction of plastic phenomena to enhance the recovery of cognitive deficits. Preoperative cortical

stimulation and behavioral training in patients with gliomas in eloquent areas has been shown to accelerate plastic changes [163], allowing for supramarginal tumor resection, improved post-surgical outcome and overall survival.

This work contributed to the advancement of our understanding of the complex phenomenon of language reorganization in the setting of brain tumors. Through our analyses, we explored neurobiological mechanisms of plasticity, common associations with patients' demographics, tumor genetics and location, as well as the specific modifications of the language network underlying plastic phenomena. Future developments will focus on promoting plastic changes through non-invasive stimulation techniques, such as TMS, and on the correlation with postsurgical outcomes.

7 REFERENCES

1. Tremblay, P.; Dick, A.S. Broca and Wernicke Are Dead, or Moving Past the Classic Model of Language Neurobiology. *Brain Lang* **2016**, *162*, 60–71, doi:10.1016/j.bandl.2016.08.004.
2. Herbet, G.; Duffau, H. Revisiting the Functional Anatomy of the Human Brain: Toward a Meta-Networking Theory of Cerebral Functions. *Physiol Rev* **2020**, *100*, 1181–1228, doi:10.1152/physrev.00033.2019.
3. Pan, C.; Peck, K.K.; Young, R.J.; Holodny, A.I. Somatotopic Organization of Motor Pathways in the Internal Capsule: A Probabilistic Diffusion Tractography Study. *American Journal of Neuroradiology* **2012**, *33*, 1274–1280, doi:10.3174/ajnr.A2952.
4. Jenabi, M.; Peck, K.K.; Young, R.J.; Brennan, N.; Holodny, A.I. Identification of the Corticobulbar Tracts of the Tongue and Face Using Deterministic and Probabilistic DTI Fiber Tracking in Patients with Brain Tumor. *American Journal of Neuroradiology* **2015**, *36*, 2036–2041, doi:10.3174/ajnr.A4430.
5. Jenabi, M.; Peck, K.K.; Young, R.J.; Brennan, N.; Holodny, A.I. Probabilistic Fiber Tracking of the Language and Motor White Matter Pathways of the Supplementary Motor Area (SMA) in Patients with Brain Tumors. *Journal of Neuroradiology* **2014**, *41*, 342–349, doi:10.1016/j.neurad.2013.12.001.
6. Tillet, Y.; Chalon, S. Brain Plasticity from Fundamental Research to Clinic. *J Chem Neuroanat* **2018**, *89*, 51–52, doi:10.1016/j.jchemneu.2018.03.004.
7. Petrovich, N.M.; Holodny, A.I.; Brennan, C.W.; Gutin, P.H. Isolated Translocation of Wernicke's Area to the Right Hemisphere in a 62-Year-Man with a Temporo-Parietal Glioma. *American Journal of Neuroradiology* **2004**, *25*, 130–133.
8. Holodny, A.I.; Schulder, M.; Ybasco, A.; Liu, W.C. Translocation of Broca's Area to the Contralateral Hemisphere as the Result of the Growth of a Left Inferior Frontal Glioma. *J Comput Assist Tomogr* **2002**, *26*, 941–943, doi:10.1097/00004728-200211000-00014.

9. Krieg, S.M.; Sollmann, N.; Hauck, T.; Ille, S.; Foerschler, A.; Meyer, B.; Ringel, F. Functional Language Shift to the Right Hemisphere in Patients with Language-Eloquent Brain Tumors. *PLoS One* **2013**, *8*, e75403, doi:10.1371/journal.pone.0075403.
10. Labudda, K.; Mertens, M.; Janszky, J.; Bien, C.G.; Woermann, F.G. Atypical Language Lateralisation Associated with Right Fronto-Temporal Grey Matter Increases - a Combined FMRI and VBM Study in Left-Sided Mesial Temporal Lobe Epilepsy Patients. *Neuroimage* **2012**, *59*, 728–737, doi:10.1016/j.neuroimage.2011.07.053.
11. Mbwana, J.; Berl, M.M.; Ritzl, E.K.; Rosenberger, L.; Mayo, J.; Weinstein, S.; Conry, J.A.; Pearl, P.L.; Shamim, S.; Moore, E.N.; et al. Limitations to Plasticity of Language Network Reorganization in Localization Related Epilepsy. *Brain* **2009**, *132*, 347–356, doi:10.1093/brain/awn329.
12. Rosenberger, L.R.; Zeck, J.; Berl, M.M.; Moore, E.N.; Ritzl, E.K.; Shamim, S.; Weinstein, S.L.; Conry, J.A.; Pearl, P.L.; Sato, S.; et al. Interhemispheric and Intrahemispheric Language Reorganization in Complex Partial Epilepsy. *Neurology* **2009**, *72*, 1830–1836, doi:10.1212/WNL.0b013e3181a7114b.
13. Turkeltaub, P.E.; Messing, S.; Norise, C.; Hamilton, R.H. Are Networks for Residual Language Function and Recovery Consistent across Aphasic Patients? *Neurology* **2011**, *76*, 1726–1734, doi:10.1212/WNL.0b013e31821a44c1.
14. Li, Q.; Dong, J.W.; Ferraro, G. del; Brennan, N.P.; Peck, K.K.; Tabar, V.; Makse, H.A.; Holodny, A.I. Functional Translocation of Broca's Area in a Low-Grade Left Frontal Glioma: Graph Theory Reveals the Novel, Adaptive Network Connectivity. *Front Neurol* **2019**, *10*, 1–6, doi:10.3389/fneur.2019.00702.
15. Desmurget, M.; Bonnetblanc, F.; Duffau, H. Contrasting Acute and Slow-Growing Lesions: A New Door to Brain Plasticity. *Brain* **2007**, *130*, 898–914, doi:10.1093/brain/awl300.
16. Brennan, N.P.; Peck, K.K.; Holodny, A. Language Mapping Using FMRI and Direct Cortical Stimulation for Brain Tumor Surgery the Good, the Bad, and the Questionable. *Topics in Magnetic Resonance Imaging* **2016**, *25*, 1–9, doi:10.1097/RMR.0000000000000074.
17. Bullmore, E.; Sporns, O. Complex Brain Networks: Graph Theoretical Analysis of Structural and Functional Systems. *Nat Rev Neurosci* **2009**, *10*, 186–198, doi:10.1038/nrn2575.
18. Gupta, A.; Shah, A.; Young, R.J.; Holodny, A.I. Imaging of Brain Tumors: Functional Magnetic Resonance Imaging and Diffusion Tensor Imaging. *Neuroimaging Clin N Am* **2010**, *20*, 379–400, doi:10.1016/j.nic.2010.04.004.
19. Dick, A.S.; Bernal, B.; Tremblay, P. The Language Connectome: New Pathways, New Concepts. *Neuroscientist* **2014**, *20*, 453–467, doi:10.1177/1073858413513502.
20. Chang, E.F.; Raygor, K.P.; Berger, M.S. Contemporary Model of Language Organization: An Overview for Neurosurgeons. *J Neurosurg* **2015**, *122*, 250–261, doi:10.3171/2014.10.JNS132647.
21. Catani, M.; Mesulam, M.M.; Jakobsen, E.; Malik, F.; Martersteck, A.; Wieneke, C.; Thompson, C.K.; Thiebaut De Schotten, M.; Dell'Acqua, F.; Weintraub, S.; et al. A Novel Frontal Pathway Underlies Verbal Fluency in Primary Progressive Aphasia. *Brain* **2013**, *136*, 2619–2628, doi:10.1093/brain/awt163.
22. Rech, F.; Herbet, G.; Gaudeau, Y.; Mézières, S.; Moureau, J.M.; Moritz-Gasser, S.; Duffau, H. A Probabilistic Map of Negative Motor Areas of the Upper Limb and Face: A Brain Stimulation Study. *Brain* **2019**, *142*, 952–965, doi:10.1093/brain/awz021.
23. Petrovich, N.; Holodny, A.I.; Tabar, V.; Correa, D.D.; Hirsch, J.; Gutin, P.H.; Brennan, C.W. Discordance between Functional Magnetic Resonance Imaging during Silent Speech Tasks and Intraoperative Speech Arrest. *J Neurosurg* **2005**, *103*, 267–274, doi:10.3171/jns.2005.103.2.0267.

24. van Geemen, K.; Herbet, G.; Moritz-Gasser, S.; Duffau, H. Limited Plastic Potential of the Left Ventral Premotor Cortex in Speech Articulation: Evidence From Intraoperative Awake Mapping in Glioma Patients. *Hum Brain Mapp* **2014**, *35*, 1587–1596, doi:10.1002/hbm.22275.
25. Friederici, A.D. The Brain Basis of Language Processing: From Structure to Function. *Physiol Rev* **2011**, *91*, 1357–1392, doi:10.1152/physrev.00006.2011.
26. Duffau, H.; Herbet, G.; Moritz-Gasser, S. Toward a Pluri-Component, Multimodal, and Dynamic Organization of the Ventral Semantic Stream in Humans: Lessons from Stimulation Mapping in Awake Patients. *Front Syst Neurosci* **2013**, *7*, 1–4, doi:10.3389/fnsys.2013.00044.
27. Pasquini, L.; di Napoli, A.; Rossi-Espagnet, M.C.; Visconti, E.; Napolitano, A.; Romano, A.; Bozzao, A.; Peck, K.K.; Holodny, A.I. Understanding Language Reorganization with Neuroimaging: How Language Adapts to Different Focal Lesions. Insights into Clinical Applications. *Front Hum Neurosci* **2022**, *epub*.
28. Tate, M.C.; Herbet, G.; Moritz-Gasser, S.; Tate, J.E.; Duffau, H. Probabilistic Map of Critical Functional Regions of the Human Cerebral Cortex: Broca's Area Revisited. *Brain* **2014**, *137*, 2773–2782, doi:10.1093/brain/awu168.
29. Sanai, N.; Mirzadeh, Z.; Berger, M.S. Functional Outcome after Language Mapping for Glioma Resection. *New England Journal of Medicine* **2008**, *358*, 18–27, doi:10.1056/nejmoa067819.
30. Smits, M.; Visch-brink, E.; Schraa-tam, C.K. Functional MR Imaging of Language Processing: An Overview of Easy-to-Implement Paradigms for Patient Care and Clinical Research. *Radiographics* **2006**, *26*, 145–159.
31. Roux, F.E.; Draper, L.; Köpke, B.; Démonet, J.F. Who Actually Read Exner? Returning to the Source of the Frontal " Writing Centre" Hypothesis. *Cortex* **2010**, *46*, 1204–1210, doi:10.1016/j.cortex.2010.03.001.
32. Matsuo, K.; Kato, C.; Sumiyoshi, C.; Toma, K.; Duy Thuy, D.H.; Moriya, T.; Fukuyama, H.; Nakai, T. Discrimination of Exner's Area and the Frontal Eye Field in Humans - Functional Magnetic Resonance Imaging during Language and Saccade Tasks. *Neurosci Lett* **2003**, *340*, 13–16, doi:10.1016/S0304-3940(03)00050-8.
33. Benjamin, C.F.; Walshaw, P.D.; Hale, K.; Gaillard, W.D.; Baxter, L.C.; Berl, M.M.; Polczynska, M.; Noble, S.; Alkawadri, R.; Hirsch, L.J.; et al. Presurgical Language FMRI: Mapping of Six Critical Regions. *Hum Brain Mapp* **2017**, *38*, 4239–4255, doi:10.1002/hbm.23661.
34. Lyo, J.K.; Arevalo-Perez, J.; Petrovich Brennan, N.; Peck, K.K.; Holodny, A.I. Pre-Operative FMRI Localization of the Supplementary Motor Area and Its Relationship with Postoperative Speech Deficits. *Neuroradiology Journal* **2015**, *28*, 281–288, doi:10.1177/1971400915589681.
35. Corrivetti, F.; de Schotten, M.T.; Poisson, I.; Froelich, S.; Descoteaux, M.; Rheault, F.; Mandonnet, E. Dissociating Motor–Speech from Lexico-Semantic Systems in the Left Frontal Lobe: Insight from a Series of 17 Awake Intraoperative Mappings in Glioma Patients. *Brain Struct Funct* **2019**, *224*, 1151–1165, doi:10.1007/s00429-019-01827-7.
36. Pattamadilok, C.; Ponz, A.; Planton, S.; Bonnard, M. Contribution of Writing to Reading: Dissociation between Cognitive and Motor Process in the Left Dorsal Premotor Cortex. *Hum Brain Mapp* **2016**, *37*, 1531–1543, doi:10.1002/hbm.23118.
37. Dong, J.W.; Brennan, N.M.P.; Izzo, G.; Peck, K.K.; Holodny, A.I. FMRI Activation in the Middle Frontal Gyrus as an Indicator of Hemispheric Dominance for Language in Brain Tumor Patients: A Comparison with Broca's Area. *Neuroradiology* **2016**, *58*, 513–520, doi:10.1007/s00234-016-1655-4.

38. Sarubbo, S.; Tate, M.; de Benedictis, A.; Merler, S.; Moritz-Gasser, S.; Herbet, G.; Duffau, H. Mapping Critical Cortical Hubs and White Matter Pathways by Direct Electrical Stimulation: An Original Functional Atlas of the Human Brain. *Neuroimage* **2020**, *205*, 116237, doi:10.1016/j.neuroimage.2019.116237.
39. Mandonnet, E. A Surgical Approach to the Anatomo-Functional Structure of Language. *Neurochirurgie* **2017**, *63*, 122–128, doi:10.1016/j.neuchi.2016.10.004.
40. Balsamo, L.M.; Xu, B.; Gaillard, W.D. Language Lateralization and the Role of the Fusiform Gyrus in Semantic Processing in Young Children. *Neuroimage* **2006**, *31*, 1306–1314, doi:10.1016/j.neuroimage.2006.01.027.
41. da Costa, S.; van der Zwaag, W.; Marques, J.P.; Frackowiak, R.S.J.; Clarke, S.; Saenz, M. Human Primary Auditory Cortex Follows the Shape of Heschl's Gyrus. *Journal of Neuroscience* **2011**, *31*, 14067–14075, doi:10.1523/JNEUROSCI.2000-11.2011.
42. Shaw, K.; Brennan, N.; Woo, K.; Zhang, Z.; Young, R.; Peck, K.; Holodny, A. Infiltration of the Basal Ganglia by Brain Tumors Is Associated with the Development of Co-Dominant Language Function on FMRI. *Brain Lang* **2016**, *155–156*, 44–48, doi:10.1016/j.bandl.2016.04.002.
43. Cappa, S.F. Imaging Semantics and Syntax. *Neuroimage* **2012**, *61*, 427–431, doi:10.1016/j.neuroimage.2011.10.006.
44. Li, Y.; Li, P.; Yang, Q.X.; Eslinger, P.J.; Sica, C.T.; Karunanayaka, P. Lexical-Semantic Search under Different Covert Verbal Fluency Tasks: An FMRI Study. *Front Behav Neurosci* **2017**, *11*, 1–15, doi:10.3389/fnbeh.2017.00131.
45. Price, C.J. A Review and Synthesis of the First 20years of PET and FMRI Studies of Heard Speech, Spoken Language and Reading. *Neuroimage* **2012**, *62*, 816–847, doi:10.1016/j.neuroimage.2012.04.062.
46. Mariën, P.; Ackermann, H.; Adamaszek, M.; Barwood, C.H.S.; Beaton, A.; Desmond, J.; de Witte, E.; Fawcett, A.J.; Hertrich, I.; Küper, M.; et al. Consensus Paper: Language and the Cerebellum: An Ongoing Enigma. *Cerebellum* **2014**, *13*, 386–410, doi:10.1007/s12311-013-0540-5.
47. Li, Q.; del Ferraro, G.; Pasquini, L.; Peck, K.K.; Makse, H.A.; Holodny, A.I. Core Language Brain Network for FMRI Language Task Used in Clinical Applications. *Network Neuroscience* **2020**, *4*, 134–154, doi:10.1162/netn_a_00112.
48. del Ferraro, G.; Moreno, A.; Min, B.; Morone, F.; Pérez-Ramírez, Ú.; Pérez-Cervera, L.; Parra, L.C.; Holodny, A.; Canals, S.; Makse, H.A. Finding Influential Nodes for Integration in Brain Networks Using Optimal Percolation Theory. *Nat Commun* **2018**, *9*, 2274, doi:10.1038/s41467-018-04718-3.
49. Morone, F.; Makse, H.A. Influence Maximization in Complex Networks through Optimal Percolation. *Nature* **2015**, *524*, 65–68, doi:10.1038/nature14604.
50. Li, Q.; Pasquini, L.; Ferraro, G. del; Gene, M.; Peck, K.K.; Makse, H.A.; Holodny, A.I. Monolingual and Bilingual Language Networks in Healthy Subjects Using Functional MRI and Graph Theory. *ArXiv* **2019**, 0–14.
51. Dan, Y.; Poo, M.M. Spike Timing-Dependent Plasticity of Neural Circuits. *Neuron* **2004**, *44*, 23–30, doi:10.1016/j.neuron.2004.09.007.
52. Ganguly, K.; Poo, M. ming Activity-Dependent Neural Plasticity from Bench to Bedside. *Neuron* **2013**, *80*, 729–741, doi:10.1016/j.neuron.2013.10.028.
53. Butz, M.; Wörgötter, F.; Ooyen, A. van Activity-Dependent Structural Plasticity. *Brain Res Rev* **2009**, *60*, 287–305, doi:10.1016/j.brainresrev.2008.12.023.
54. Sakai, J. How Synaptic Pruning Shapes Neural Wiring during Development and, Possibly, in Disease. *Proc Natl Acad Sci U S A* **2020**, *117*, 16096–16099, doi:10.1073/pnas.2010281117.

55. Sampaio-Baptista, C.; Johansen-Berg, H. White Matter Plasticity in the Adult Brain. *Neuron* **2017**, *96*, 1239–1251, doi:10.1016/j.neuron.2017.11.026.
56. Kempermann, G.; Wiskott, L.; Gage, F.H. Functional Significance of Adult Neurogenesis. *Curr Opin Neurobiol* **2004**, *14*, 186–191, doi:10.1016/j.conb.2004.03.001.
57. Sailor, K.A.; Schinder, A.F.; Lledo, P.M. Adult Neurogenesis beyond the Niche: Its Potential for Driving Brain Plasticity. *Curr Opin Neurobiol* **2017**, *42*, 111–117, doi:10.1016/j.conb.2016.12.001.
58. Andreae, L.C.; Burrone, J. The Role of Neuronal Activity and Transmitter Release on Synapse Formation. *Curr Opin Neurobiol* **2014**, *27*, 47–52, doi:10.1016/j.conb.2014.02.008.
59. Iadecola, C. The Neurovascular Unit Coming of Age: A Journey through Neurovascular Coupling in Health and Disease. *Neuron* **2017**, *96*, 17–42, doi:10.1016/j.neuron.2017.07.030.
60. Dhuriya, Y.K.; Sharma, D. Neuronal Plasticity: Neuronal Organization Is Associated with Neurological Disorders. *Journal of Molecular Neuroscience* **2020**, *70*, 1684–1701, doi:10.1007/s12031-020-01555-2.
61. Draganski, B.; Gaser, C.; Busch, V.; Schuierer, G.; Bogdahn, U.; May, A. Changes in Grey Matter Induced by Training. *Nature* **2004**, *427*, 311–312, doi:10.1038/427311a.
62. Draganski, B.; Gaser, C.; Kempermann, G.; Kuhn, H.G.; Winkler, J.; Büchel, C.; May, A. Temporal and Spatial Dynamics of Brain Structure Changes during Extensive Learning. *J Neurosci* **2006**, *26*, 6314–6317, doi:10.1523/JNEUROSCI.4628-05.2006.
63. Takao, H.; Abe, O.; Ohtomo, K. Computational Analysis of Cerebral Cortex. *Neuroradiology* **2010**, *52*, 691–698, doi:10.1007/s00234-010-0715-4.
64. Timmers, I.; Roebroeck, A.; Bastiani, M.; Jansma, B.; Rubio-Gozalbo, E.; Zhang, H. Assessing Microstructural Substrates of White Matter Abnormalities: A Comparative Study Using DTI and NODDI. *PLoS One* **2016**, *11*, 1–15, doi:10.1371/journal.pone.0167884.
65. Sato, K.; Kerever, A.; Kamagata, K.; Tsuruta, K.; Irie, R.; Tagawa, K.; Okazawa, H.; Arikawa-Hirasawa, E.; Nitta, N.; Aoki, I.; et al. Understanding Microstructure of the Brain by Comparison of Neurite Orientation Dispersion and Density Imaging (NODDI) with Transparent Mouse Brain. *Acta Radiol Open* **2017**, *6*, 205846011770381, doi:10.1177/2058460117703816.
66. Ribic, A.; Biederer, T.; Morishita, H. Emerging Roles of Synapse Organizers in the Regulation of Critical Periods. *Neural Plast* **2019**, *2019*, 1538137, doi:10.1155/2019/1538137.
67. Nahmani, M.; Turrigiano, G.G. Adult Cortical Plasticity Following Injury: Recapitulation of Critical Period Mechanisms? *Neuroscience* **2014**, *283*, 4–16, doi:10.1016/j.neuroscience.2014.04.029.
68. Ovsepian, S. v The Dark Matter of the Brain. *Brain Struct Funct* **2019**, *224*, 973–983, doi:10.1007/s00429-019-01835-7.
69. Dancause, N.; Barbay, S.; Frost, S.B.; Plautz, E.J.; Chen, D.; Zoubina, E. v.; Stowe, A.M.; Nudo, R.J. Extensive Cortical Rewiring after Brain Injury. *Journal of Neuroscience* **2005**, *25*, 10167–10179, doi:10.1523/JNEUROSCI.3256-05.2005.
70. Isaacs, K.L.; Barr, W.B.; Nelson, P.K.; Devinsky, O. Degree of Handedness and Cerebral Dominance. *Neurology* **2006**, *66*, 1855–1858, doi:10.1212/01.wnl.0000219623.28769.74.
71. Knecht, S.; Drager, M.; Deppe, L.; Bobe, H.; Lohmann, A.; Ringelstein, E.B.; Henningsen, H. Handedness and Hemispheric Language Dominance in Healthy Humans. *Brain* **2000**, *123*, 2512–2518, doi:10.1093/brain/123.12.2512.
72. Hartwigsen, G.; Bzdok, D.; Klein, M.; Wawrzyniak, M.; Stockert, A.; Wrede, K.; Classen, J.; Saur, D. Rapid Short-Term Reorganization in the Language Network. *Elife* **2017**, *6*, 1–18, doi:10.7554/elife.25964.

73. Tantillo, G.; Peck, K.K.; Arevalo-Perez, J.; Lyo, J.K.; Chou, J.F.; Young, R.J.; Petrovich-Brennan, N.M.; Holodny, A.I. Corpus Callosum Diffusion and Language Lateralization in Patients with Brain Tumors: A DTI and FMRI Study. *Journal of Neuroimaging* **2016**, *26*, 224–231, doi:10.1111/jon.12275.Corpus.
74. Briganti, C.; Sestieri, C.; Mattei, P.A.; Esposito, R.; Galzio, R.J.; Tartaro, A.; Romani, G.L.; Caulo, M. Reorganization of Functional Connectivity of the Language Network in Patients with Brain Gliomas. *American Journal of Neuroradiology* **2012**, *33*, 1983–1990, doi:10.3174/ajnr.A3064.
75. Duffau, H. Hodotopy, Neuroplasticity and Diffuse Gliomas. *Neurochirurgie* **2017**, *63*, 259–265, doi:10.1016/j.neuchi.2016.12.001.
76. Salek, K. el; Hassan, I.S.; Kotrotsou, A.; Abrol, S.; Faro, S.H.; Mohamed, F.B.; Zinn, P.O.; Wei, W.; Li, N.; Kumar, A.J.; et al. Silent Sentence Completion Shows Superiority Localizing Wernicke's Area and Activation Patterns of Distinct Language Paradigms Correlate with Genomics: Prospective Study. *Sci Rep* **2017**, *7*, 1–8, doi:10.1038/s41598-017-11192-2.
77. Gratton, C.; Nomura, E.M.; Pérez, F.; D'Esposito, M. Focal Brain Lesions to Critical Locations Cause Widespread Disruption of the Modular Organization of the Brain. *J Cogn Neurosci* **2012**, *24*, 1275–1285, doi:10.1162/jocn_a_00222.
78. Duffau, H.; Capelle, L.; Denvil, D.; Sichez, N.; Gatignol, P.; Lopes, M.; Mitchell, M.C.; Sichez, J.P.; van Effenterre, R. Functional Recovery after Surgical Resection of Low Grade Gliomas in Eloquent Brain: Hypothesis of Brain Compensation. *J Neurol Neurosurg Psychiatry* **2003**, *74*, 901–907, doi:10.1136/jnnp.74.7.901.
79. Gębska-Kośla, K.; Bryszewski, B.; Jaskólski, D.J.; Fortuniak, J.; Niewodniczy, M.; Stefańczyk, L.; Majos, A. Reorganization of Language Centers in Patients with Brain Tumors Located in Eloquent Speech Areas – A Pre- and Postoperative Preliminary FMRI Study. *Neurol Neurochir Pol* **2017**, *51*, 403–410, doi:10.1016/j.pjnns.2017.07.010.
80. Wang, L.; Chen, D.; Yang, X.; Olson, J.J.; Gopinath, K.; Fan, T.; Mao, H. Group Independent Component Analysis and Functional MRI Examination of Changes in Language Areas Associated with Brain Tumors at Different Locations. *PLoS One* **2013**, *8*, 1–10, doi:10.1371/journal.pone.0059657.
81. Rosenberg, K.; Liebling, R.; Avidan, G.; Perry, D.; Siman-Tov, T.; Andelman, F.; Ram, Z.; Fried, I.; Hendler, T. Language Related Reorganization in Adult Brain with Slow Growing Glioma: FMRI Prospective Case-Study. *Neurocase* **2008**, *14*, 465–473, doi:10.1080/13554790802459486.
82. Duffau, H. Lessons from Brain Mapping in Surgery for Low-Grade Glioma: Insights into Associations between Tumour and Brain Plasticity. *Lancet Neurology* **2005**, *4*, 476–486, doi:10.1016/S1474-4422(05)70140-X.
83. Meyer, P.T.; Sturz, L.; Schreckenberger, M.; Spetzger, U.; Meyer, G.F.; Setani, K.S.; Sabri, O.; Buell, U. Preoperative Mapping of Cortical Language Areas in Adult Brain Tumour Patients Using PET and Individual Non-Normalised SPM Analyses. *Eur J Nucl Med Mol Imaging* **2003**, *30*, 951–960, doi:10.1007/s00259-003-1186-1.
84. Duffau, H.; Bauchet, L.; Lehéricy, S.; Capelle, L. Functional Compensation of the Left Dominant Insula for Language. *Neuroreport* **2001**, *12*, 2159–2163, doi:10.1097/00001756-200107200-00023.
85. Thiel, A.; Herholz, K.; Koyuncu, A.; Ghaemi, M.; Kracht, L.W.; Habedank, B.; Heiss, W.D. Plasticity of Language Networks in Patients with Brain Tumors: A Positron Emission Tomography Activation Study. *Ann Neurol* **2001**, *50*, 620–629, doi:10.1002/ana.1253.

86. Benzagmount, M.; Gatignol, P.; Duffau, H. Resection of World Health Organization Grade II Gliomas Involving Broca's Area: Methodological and Functional Considerations. *Neurosurgery* **2007**, *61*, 741–753, doi:10.1227/01.NEU.0000280069.13468.B2.
87. Kośla, K.; Pfajfer, L.; Bryszewski, B.; Jaskólski, D.; Stefańczyk, L.; Majos, A. Functional Rearrangement of Language Areas in Patients with Tumors of the Central Nervous System Using Functional Magnetic Resonance Imaging. *Pol J Radiol* **2012**, *77*, 39–45, doi:10.12659/PJR.883373.
88. Cho, N.S.; Peck, K.K.; Zhang, Z.; Holodny, A.I. Paradoxical Activation in the Cerebellum During Language FMRI in Patients with Brain Tumors: Possible Explanations Based on Neurovascular Uncoupling and Functional Reorganization. *Cerebellum* 2018, *17*, 286–293.
89. Zhang, N.; Xia, M.; Qiu, T.; Wang, X.; Lin, C. po; Guo, Q.; Lu, J.; Wu, Q.; Zhuang, D.; Yu, Z.; et al. Reorganization of Cerebro-Cerebellar Circuit in Patients with Left Hemispheric Gliomas Involving Language Network: A Combined Structural and Resting-State Functional MRI Study. *Hum Brain Mapp* **2018**, *39*, 4802–4819, doi:10.1002/hbm.24324.
90. Kong, N.W.; Gibb, W.R.; Tate, M.C. Neuroplasticity: Insights from Patients Harboring Gliomas. *Neural Plast* **2016**, *2016*, 2365063, doi:10.1155/2016/2365063.
91. Thiel, A.; Habedank, B.; Winhuisen, L.; Herholz, K.; Kessler, J.; Haupt, W.F.; Heiss, W.D. Essential Language Function of the Right Hemisphere in Brain Tumor Patients. *Ann Neurol* **2005**, *57*, 128–131, doi:10.1002/ana.20342.
92. Rösler, J.; Niraula, B.; Strack, V.; Zdunczyk, A.; Schilt, S.; Savolainen, P.; Lioumis, P.; Mäkelä, J.; Vajkoczy, P.; Frey, D.; et al. Language Mapping in Healthy Volunteers and Brain Tumor Patients with a Novel Navigated TMS System: Evidence of Tumor-Induced Plasticity. *Clinical Neurophysiology* **2014**, *125*, 526–536, doi:10.1016/j.clinph.2013.08.015.
93. Lubrano, V.; Draper, L.; Roux, F.E. What Makes Surgical Tumor Resection Feasible in Broca's Area? Insights into Intraoperative Brain Mapping. *Neurosurgery* **2010**, *66*, 868–875, doi:10.1227/01.NEU.0000368442.92290.04.
94. Russell, S.M.; Kelly, P.J.; Schramm, J.; Meyer, B.; Grossman, R.G.; Berger, M.S. Incidence and Clinical Evolution of Postoperative Deficits after Volumetric Stereotactic Resection of Glial Neoplasms Involving the Supplementary Motor Area. *Neurosurgery* **2003**, *52*, 506–516, doi:10.1227/01.NEU.0000047670.56996.53.
95. Sarubbo, S.; Latini, F.; Sette, E.; Milani, P.; Granieri, E.; Fainardi, E.; Cavallo, M.A. Is the Resection of Gliomas in Wernicke's Area Reliable? Wernicke's Area Resection. *Acta Neurochir (Wien)* **2012**, *154*, 1653–1662, doi:10.1007/s00701-012-1416-z.
96. Meyer, P.T.; Sturz, L.; Sabri, O.; Schreckenberger, M.; Spetzger, U.; Setani, K.S.; Kaiser, H.J.; Buell, U. Preoperative Motor System Brain Mapping Using Positron Emission Tomography and Statistical Parametric Mapping: Hints on Cortical Reorganisation. *J Neurol Neurosurg Psychiatry* **2003**, *74*, 471–478, doi:10.1136/jnnp.74.4.471.
97. Cargnelutti, E.; Ius, T.; Skrap, M.; Tomasino, B. NeuroImage : Clinical What Do We Know about Pre- and Postoperative Plasticity in Patients with Glioma ? A Review of Neuroimaging and Intraoperative Mapping Studies. *Neuroimage Clin* **2020**, *28*, 102435, doi:10.1016/j.nicl.2020.102435.
98. Kristo, G.; Raemaekers, M.; Rutten, G.J.; de Gelder, B.; Ramsey, N.F. Inter-Hemispheric Language Functional Reorganization in Low-Grade Glioma Patients after Tumour Surgery. *Cortex* **2015**, *64*, 235–248, doi:10.1016/j.cortex.2014.11.002.
99. Deverdun, J.; van Dokkum, L.E.H.; le Bars, E.; Herbet, G.; Mura, T.; D'agata, B.; Picot, M.C.; Menjot, N.; Molino, F.; Duffau, H.; et al. Language Reorganization after Resection of Low-Grade Gliomas: An FMRI Task Based Connectivity Study. *Brain Imaging Behav* **2020**, *14*, 1779–1791, doi:10.1007/s11682-019-00114-7.

100. Duffau, H. The " Frontal Syndrome" Revisited: Lessons from Electrostimulation Mapping Studies. *Cortex* 2012, *48*, 120–131.
101. Duffau, H. The Huge Plastic Potential of Adult Brain and the Role of Connectomics: New Insights Provided by Serial Mappings in Glioma Surgery. *Cortex* **2014**, *58*, 325–337, doi:10.1016/j.cortex.2013.08.005.
102. Chivukula, S.; Pikul, B.K.; Black, K.L.; Pouratian, N.; Bookheimer, S.Y. Contralateral Functional Reorganization of the Speech Supplementary Motor Area Following Neurosurgical Tumor Resection. *Brain Lang* **2018**, *183*, 41–46, doi:10.1016/j.bandl.2018.05.006.
103. Krainik, A.; Duffau, H.; Capelle, L.; Cornu, P.; Boch, A.L.; Mangin, J.F.; le Bihan, D.; Marsault, C.; Chiras, J.; Lehéricy, S. Role of the Healthy Hemisphere in Recovery after Resection of the Supplementary Motor Area. *Neurology* **2004**, *62*, 1323–1332, doi:10.1212/01.WNL.0000120547.83482.B1.
104. Miotto, E.C.; Balardin, J.B.; Vieira, G.; Sato, J.R.; Martin, M.D.G.M.; Scaff, M.; Teixeira, M.J.; Amaro, E. Right Inferior Frontal Gyrus Activation Is Associated with Memory Improvement in Patients with Left Frontal Low-Grade Glioma Resection. *PLoS One* **2014**, *9*, e105987, doi:10.1371/journal.pone.0105987.
105. Gabriel, M.; Brennan, N.P.; Peck, K.K.; Holodny, A.I. Blood Oxygen Level Dependent Functional Magnetic Resonance Imaging for Presurgical Planning. *Neuroimaging Clin N Am* **2014**, *24*, 557–571, doi:10.1016/j.nic.2014.07.003.
106. Petrella, J.R.; Shah, L.M.; Harris, K.M.; Friedman, A.H.; George, T.M.; Sampson, J.H.; Pekala, J.S.; Voyvodic, J.T. Preoperative Functional MR Imaging Localization of Language and Motor Areas: Effect on Therapeutic Decision Making in Patients with Potentially Resectable Brain Tumors. *Radiology* **2006**, *240*, 793–802, doi:10.1148/radiol.2403051153.
107. Molinaro, A.M.; Hervey-Jumper, S.; Morshed, R.A.; Young, J.; Han, S.J.; Chunduru, P.; Zhang, Y.; Phillips, J.J.; Shai, A.; Lafontaine, M.; et al. Association of Maximal Extent of Resection of Contrast-Enhanced and Non-Contrast-Enhanced Tumor with Survival Within Molecular Subgroups of Patients with Newly Diagnosed Glioblastoma. *JAMA Oncol* **2020**, *6*, 495–503, doi:10.1001/jamaoncol.2019.6143.
108. Roux, F.E.; Djidjeli, I.; Quéhan, R.; Réhault, E.; Giussani, C.; Durand, J.B. Intraoperative Electrostimulation for Awake Brain Mapping: How Many Positive Interference Responses Are Required for Reliability? *J Neurosurg* **2020**, *133*, 1191–1201, doi:10.3171/2019.6.JNS19925.
109. Belyaev, A.S.; Peck, K.K.; Petrovich Brennan, N.M.; Holodny, A.I. Clinical Applications of Functional MR Imaging. *Magn Reson Imaging Clin N Am* **2013**, *21*, 269–278, doi:10.1016/j.mric.2012.12.001.
110. Sopich, N.; Holodny, A.I. Introduction to Functional MR Imaging. *Neuroimaging Clin N Am* **2021**, *31*, 1–10, doi:10.1016/j.nic.2020.09.002.
111. Black, D.F.; Vachha, B.; Mian, A.; Faro, S.H.; Maheshwari, M.; Sair, H.I.; Petrella, J.R.; Pillai, J.J.; Welker, K. American Society of Functional Neuroradiology-Recommended FMRI Paradigm Algorithms for Presurgical Language Assessment. *American Journal of Neuroradiology* **2017**, *38*, E65–E73, doi:10.3174/ajnr.A5345.
112. Luna, L.P.; Sherbaf, F.G.; Sair, H.I.; Mukherjee, D.; Oliveira, I.B.; Köhler, C.A. Can Preoperative Mapping with Functional MRI Reduce Morbidity in Brain Tumor Resection? A Systematic Review and Meta-Analysis of 68 Observational Studies. *Radiology* **2021**, *300*, 338–349, doi:10.1148/radiol.2021204723.
113. Rosenberg, K.; Liebling, R.; Avidan, G.; Perry, D.; Siman-Tov, T.; Andelman, F.; Ram, Z.; Fried, I.; Hendler, T. Language Related Reorganization in Adult Brain with Slow Growing

Glioma: FMRI Prospective Case-Study. *Neurocase* **2008**, *14*, 465–473, doi:10.1080/13554790802459486.
114. Duffau, H. Diffuse Low-Grade Gliomas and Neuroplasticity. *Diagn Interv Imaging* **2014**, *95*, 945–955, doi:10.1016/j.diii.2014.08.001.
115. Stensjøen, A.L.; Berntsen, E.M.; Jakola, A.S.; Solheim, O. When Did the Glioblastoma Start Growing, and How Much Time Can Be Gained from Surgical Resection? A Model Based on the Pattern of Glioblastoma Growth in Vivo. *Clin Neurol Neurosurg* **2018**, *170*, 38–42, doi:10.1016/j.clineuro.2018.04.028.
116. Mårtensson, J.; Eriksson, J.; Bodammer, N.C.; Lindgren, M.; Johansson, M.; Nyberg, L.; Lövdén, M. Growth of Language-Related Brain Areas after Foreign Language Learning. *Neuroimage* **2012**, *63*, 240–244, doi:10.1016/j.neuroimage.2012.06.043.
117. Maguire, E.A.; Gadian, D.G.; Johnsrude, I.S.; Good, C.D.; Ashburner, J.; Frackowiak, R.S.J.; Frith, C.D. Navigation-Related Structural Change in the Hippocampi of Taxi Drivers. *Proc Natl Acad Sci U S A* **2000**, *97*, 4398–4403, doi:10.1073/pnas.070039597.
118. Bassett, D.S.; Bullmore, E.T. Human Brain Networks in Health and Disease. *Curr Opin Neurol* **2009**, *22*, 340–347, doi:10.1097/WCO.0b013e32832d93dd.
119. Bullmore, E.; Sporns, O. Complex Brain Networks: Graph Theoretical Analysis of Structural and Functional Systems. *Nat Rev Neurosci* **2009**, *10*, 186–198, doi:10.1038/nrn2575.
120. Bottino, F.; Lucignani, M.; Pasquini, L.; Mastrogiovanni, M.; Gazzellini, S.; Ritrovato, M.; Longo, D.; Figà-Talamanca, L.; Rossi Espagnet, M.C.; Napolitano, A. Spatial Stability of Functional Networks: A Measure to Assess the Robustness of Graph-Theoretical Metrics to Spatial Errors Related to Brain Parcellation. *Front Neurosci* **2022**, *15*, 1–18, doi:10.3389/fnins.2021.736524.
121. Pasquini, L.; Jenabi, M.; Yildirim, O.; Silveira, P.; Peck, K.K.; Holodny, A.I. Brain Functional Connectivity in Low- and High-Grade Gliomas : Differences in Network Dynamics Associated with Tumor Grade and Location. *Cancers (Basel)* **2022**, *14*, 3327, doi:10.3390/cancers14143327.
122. Morone, F.; del Ferraro, G.; Makse, H.A. The K-Core as a Predictor of Structural Collapse in Mutualistic Ecosystems. *Nat Phys* **2019**, *15*, 95–102, doi:10.1038/s41567-018-0304-8.
123. Li, Q.; Pasquini, L.; del Ferraro, G.; Gene, M.; Peck, K.K.; Makse, H.A.; Holodny, A.I. Monolingual and Bilingual Language Networks in Healthy Subjects Using Functional MRI and Graph Theory. *Sci Rep* **2021**, *11*, 1–14, doi:10.1038/s41598-021-90151-4.
124. Oldfield, R.C. The Assessment and Analysis of Handedness: The Edinburgh Inventory. *Neuropsychologia* **1971**, *9*, 97–113, doi:10.1016/0028-3932(71)90067-4.
125. Cheng, D.T.; Mitchell, T.N.; Zehir, A.; Shah, R.H.; Benayed, R.; Syed, A.; Chandramohan, R.; Liu, Z.Y.; Won, H.H.; Scott, S.N.; et al. Memorial Sloan Kettering-Integrated Mutation Profiling of Actionable Cancer Targets (MSK-IMPACT): A Hybridization Capture-Based next-Generation Sequencing Clinical Assay for Solid Tumor Molecular Oncology. *Journal of Molecular Diagnostics* **2015**, *17*, 251–264, doi:10.1016/j.jmoldx.2014.12.006.
126. Kaplan, E.; Goodglass, H.; Weintraub, S. *Boston Naming Test*; 2nd ed.; Philadelphia : Lea & Febiger, 1983;
127. Benton, A.L.; Kerry, H. des; Sivan, A.B. *Multilingual Aphasia Examination*; Iowa City: University of Iowa, 1976;
128. Louis, D.N.; Perry, A.; Reifenberger, G.; von Deimling, A.; Figarella-Branger, D.; Cavenee, W.K.; Ohgaki, H.; Wiestler, O.D.; Kleihues, P.; Ellison, D.W. The 2016 World Health Organization Classification of Tumors of the Central Nervous System: A Summary. *Acta Neuropathol* **2016**, *131*, 803–820, doi:10.1007/s00401-016-1545-1.
129. Tonn, J.C. Awake Craniotomy for Monitoring of Language Function: Benefits and Limits. *Acta Neurochir (Wien)* **2007**, *149*, 1197–1198, doi:10.1007/s00701-007-1368-x.

130. Cox, R.W. AFNI: Software for Analysis and Visualization of Functional Magnetic Resonance Neuroimages. *Computers and Biomedical Research* **1996**, *29*, 162–173, doi:10.1006/cbmr.1996.0014.
131. Fernández, G.; Specht, K.; Weis, S.; Tendolkar, I.; Reuber, M.; Fell, J.; Klaver, P.; Ruhlmann, J.; Reul, J.; Elger, C.E. Intrasubject Reproducibility of Presurgical Language Lateralization and Mapping Using FMRI. *Neurology* **2003**, *60*, 969–975, doi:10.1212/01.WNL.0000049934.34209.2E.
132. Fernández, G.; de Greiff, A.; von Oertzen, J.; Reuber, M.; Lun, S.; Klaver, P.; Ruhlmann, J.; Reul, J.; Elger, C.E. Language Mapping in Less than 15 Minutes: Real-Time Functional MRI during Routine Clinical Investigation. *Neuroimage* **2001**, *14*, 585–594, doi:10.1006/nimg.2001.0854.
133. Arese Lucini, F.; del Ferraro, G.; Sigman, M.; Makse, H.A. How the Brain Transitions from Conscious to Subliminal Perception. *Neuroscience* **2019**, *411*, 280–290, doi:10.1016/j.neuroscience.2019.03.047.
134. Whitfield-Gabrieli, S.; Nieto-Castanon, A. Conn: A Functional Connectivity Toolbox for Correlated and Anticorrelated Brain Networks. *Brain Connect* **2012**, *2*, 125–141, doi:10.1089/brain.2012.0073.
135. Latora, V.; Marchiori, M. Efficient Behavior of Small-World Networks. *Phys Rev Lett* **2001**, *87*, 198701-1-198701–198704, doi:10.1103/PhysRevLett.87.198701.
136. Douaud, G.; Smith, S.; Jenkinson, M.; Behrens, T.; Johansen-Berg, H.; Vickers, J.; James, S.; Voets, N.; Watkins, K.; Matthews, P.M.; et al. Anatomically Related Grey and White Matter Abnormalities in Adolescent-Onset Schizophrenia. *Brain* **2007**, *130*, 2375–2386, doi:10.1093/brain/awm184.
137. Good, C.D.; Johnsrude, I.S.; Ashburner, J.; Henson, R.N.A.; Friston, K.J.; Frackowiak, R.S.J. A Voxel-Based Morphometric Study of Ageing in 465 Normal Adult Human Brains. *Neuroimage* **2001**, *14*, 21–36, doi:10.1006/nimg.2001.0786.
138. Smith, S.M.; Jenkinson, M.; Woolrich, M.W.; Beckmann, C.F.; Behrens, T.E.J.; Johansen-Berg, H.; Bannister, P.R.; de Luca, M.; Drobnjak, I.; Flitney, D.E.; et al. Advances in Functional and Structural MR Image Analysis and Implementation as FSL. *Neuroimage* **2004**, *23*, 208–219, doi:10.1016/j.neuroimage.2004.07.051.
139. Winkler, A.M.; Ridgway, G.R.; Webster, M.A.; Smith, S.M.; Nichols, T.E. Permutation Inference for the General Linear Model. *Neuroimage* **2014**, *92*, 381–397, doi:10.1016/j.neuroimage.2014.01.060.
140. Desikan, R.S.; Ségonne, F.; Fischl, B.; Quinn, B.T.; Dickerson, B.C.; Blacker, D.; Buckner, R.L.; Dale, A.M.; Maguire, R.P.; Hyman, B.T.; et al. An Automated Labeling System for Subdividing the Human Cerebral Cortex on MRI Scans into Gyral Based Regions of Interest. *Neuroimage* **2006**, *31*, 968–980, doi:10.1016/j.neuroimage.2006.01.021.
141. Seghier, M.L. Laterality Index in Functional MRI: Methodological Issues. *Magn Reson Imaging* **2008**, *26*, 594–601, doi:10.1016/j.mri.2007.10.010.
142. Silver, M.; Montana, G.; Nichols, T.E. False Positives in Neuroimaging Genetics Using Voxel-Based Morphometry Data. *Neuroimage* **2011**, *54*, 992–1000, doi:10.1016/j.neuroimage.2010.08.049.
143. Roiser, J.P.; Linden, D.E.; Gorno-Tempinin, M.L.; Moran, R.J.; Dickerson, B.C.; Grafton, S.T. Minimum Statistical Standards for Submissions to Neuroimage: Clinical. *Neuroimage Clin* **2016**, *12*, 1045–1047, doi:10.1016/j.nicl.2016.08.002.
144. Bera, A.K.; Jarque, C.M. Efficient Tests for Normality, Homoscedasticity and Serial Independence of Regression Residuals. Monte Carlo Evidence. *Economic Letters* **1981**, *7*, 313–318.

145. Anderson, B.J.; Eckburg, P.B.; Relucio, K.I. Alterations in the Thickness of Motor Cortical Subregions after Motor-Skill Learning and Exercise. *Learning and Memory* **2002**, *9*, 1–9, doi:10.1101/lm.43402.
146. Hegi, M.E.; Diserens, A.-C.; Gorlia, T.; Hamou, M.-F.; de Tribolet, N.; Weller, M.; Kros, J.M.; Hainfellner, J.A.; Mason, W.; Mariani, L.; et al. MGMT Gene Silencing and Benefit from Temozolomide in Glioblastoma . *New England Journal of Medicine* **2005**, *352*, 997–1003, doi:10.1056/nejmoa043331.
147. Saadeh, F.S.; Mahfouz, R.; Assi, H.I. Egfr as a Clinical Marker in Glioblastomas and Other Gliomas. *International Journal of Biological Markers* **2018**, *33*, 22–32, doi:10.5301/ijbm.5000301.
148. Pasquini, L.; Napolitano, A.; Lucignani, M.; Tagliente, E.; Dellepiane, F.; Rossi-Espagnet, M.C.; Ritrovato, M.; Vidiri, A.; Villani, V.; Ranazzi, G.; et al. AI and High-Grade Glioma for Diagnosis and Outcome Prediction: Do All Machine Learning Models Perform Equally Well? *Front Oncol* **2021**, *11*, 1–14, doi:10.3389/fonc.2021.601425.
149. Pak, R.W.; Hadjiabadi, D.H.; Senarathna, J.; Agarwal, S.; Thakor, N. v.; Pillai, J.J.; Pathak, A.P. Implications of Neurovascular Uncoupling in Functional Magnetic Resonance Imaging (FMRI) of Brain Tumors. *Journal of Cerebral Blood Flow and Metabolism* **2017**, *37*, 3475–3487, doi:10.1177/0271678X17707398.
150. Ardizzone, A.; Scuderi, S.A.; Giuffrida, D.; Colarossi, C.; Campolo, M.; Cuzzocrea, S.; Esposito, E.; Paterniti, I. Role of Fibroblast Growth Factors Receptors (FGFRs) in Brain Tumors, Focus on Astrocytoma and Glioblastoma. *Cancers (Basel)* **2020**, *12*, 1–22, doi:10.3390/cancers12123825.
151. de Abreu, V.H.F.; Peck, K.K.; Petrovich-Brennan, N.M.; Woo, K.M.; Holodny, A.I. Brain Tumors: The Influence of Tumor Type and Routine MR Imaging Characteristics at BOLD Functional MR Imaging in the Primary Motor Gyrus. *Radiology* **2016**, *281*, 876–883, doi:10.1148/radiol.2016151951.
152. Liu, W.C.; Feldman, S.C.; Schulder, M.; Kalnin, A.J.; Holodny, A.I.; Zimmerman, A.; Sinensky, R.; Rao, S. The Effect of Tumour Type and Distance on Activation in the Motor Cortex. *Neuroradiology* **2005**, *47*, 813–819, doi:10.1007/s00234-005-1428-y.
153. Mallela, A.N.; Peck, K.K.; Petrovich-Brennan, N.M.; Zhang, Z.; Lou, W.; Holodny, A.I. Altered Resting-State Functional Connectivity in the Hand Motor Network in Glioma Patients. *Brain Connect* **2016**, *6*, 587–595, doi:10.1089/brain.2016.0432.
154. Derks, J.; Dirkson, A.R.; de Witt Hamer, P.C.; van Geest, Q.; Hulst, H.E.; Barkhof, F.; Pouwels, P.J.W.; Geurts, J.J.G.; Reijneveld, J.C.; Douw, L. Connectomic Profile and Clinical Phenotype in Newly Diagnosed Glioma Patients. *Neuroimage Clin* **2017**, *14*, 87–96, doi:10.1016/j.nicl.2017.01.007.
155. Vollmann-Zwerenz, A.; Leidgens, V.; Feliciello, G.; Klein, C.A.; Hau, P. Tumor Cell Invasion in Glioblastoma. *Int J Mol Sci* **2020**, *21*, 1–21, doi:10.3390/ijms21061932.
156. Carrera, E.; Tononi, G. Diaschisis: Past, Present, Future. *Brain* **2014**, *137*, 2408–2422, doi:10.1093/brain/awu101.
157. Friederici, A.D.; Gierhan, S.M.E. The Language Network. *Curr Opin Neurobiol* **2013**, *23*, 250–254, doi:10.1016/j.conb.2012.10.002.
158. Keidel, J.L.; Welbourne, S.R.; Lambon Ralph, M.A. Solving the Paradox of the Equipotential and Modular Brain: A Neurocomputational Model of Stroke vs. Slow-Growing Glioma. *Neuropsychologia* **2010**, *48*, 1716–1724, doi:10.1016/j.neuropsychologia.2010.02.019.
159. Sarubbo, S.; Bars, E. le; Sylvie, M.G.; Duffau, H.; Sarubbo, S. Complete Recovery after Surgical Resection of Left Wernicke's Area in Awake Patient: A Brain Stimulation and Functional MRI Study. *Neurosurg Rev* 2012, *35*, 287–292.

160. Wigmore, P. The Effect of Systemic Chemotherapy on Neurogenesis, Plasticity and Memory. *Curr Topics Behav Neurosci* **2012**, 211–240, doi:10.1007/7854_2012_235.
161. Kardan, O.; Reuter-Lorenz, P.A.; Peltier, S.; Churchill, N.W.; Misic, B.; Askren, M.K.; Jung, M.S.; Cimprich, B.; Berman, M.G. Brain Connectivity Tracks Effects of Chemotherapy Separately from Behavioral Measures. *Neuroimage Clin* **2019**, *21*, 101654, doi:10.1016/j.nicl.2019.101654.
162. Mitchell, T.J.; Seitzman, B.A.; Ballard, N.; Petersen, S.E.; Shimony, J.S.; Leuthardt, E.C. Human Brain Functional Network Organization Is Disrupted after Whole-Brain Radiation Therapy. *Brain Connect* **2020**, *10*, 29–38, doi:10.1089/brain.2019.0713.
163. Rivera-Rivera, P.A.; Rios-Lago, M.; Sanchez-Casarrubios, S.; Salazar, O.; Yus, M.; González-Hidalgo, M.; Sanz, A.; Avecillas-Chasin, J.; Alvarez-Linera, J.; Pascual-Leone, A.; et al. Cortical Plasticity Catalyzed by Prehabilitation Enables Extensive Resection of Brain Tumors in Eloquent Areas. *J Neurosurg* **2017**, *126*, 1323–1333, doi:10.3171/2016.2.JNS152485.
164. Quinones, A.; Jenabi, M.; Pasquini, L.; Peck, K.; Moss, N.S.; Brennan, C.; Tabar, V.; Holodny, A. Longitudinal Functional MRI Demonstrates Translocation of Language Function in Patients with Brain Tumors. *J Neurosurg* **2022**.
165. Saur, D.; Lange, R.; Baumgaertner, A.; Schraknepper, V.; Willmes, K.; Rijntjes, M.; Weiller, C. Dynamics of Language Reorganization after Stroke. *Brain* **2006**, *129*, 1371–1384, doi:10.1093/brain/awl090.
166. Robles, S.G.; Gatignol, P.; Lehéricy, S.; Duffau, H. Long-Term Brain Plasticity Allowing a Multistage Surgical Approach to World Health Organization Grade II Gliomas in Eloquent Areas: Report of 2 Cases. *J Neurosurg* **2008**, *109*, 615–624, doi:10.3171/JNS/2008/109/10/0615.
167. Picart, T.; Herbet, G.; Moritz-Gasser, S.; Duffau, H. Iterative Surgical Resections of Diffuse Glioma with Awake Mapping: How to Deal with Cortical Plasticity and Connectomal Constraints? *Clin Neurosurg* **2019**, *85*, 105–116, doi:10.1093/neuros/nyy218.